

**Full title:** Persistence of a reef fish metapopulation via network connectivity: theory and data

**Running title:** Empirical metapopulation persistence

**Keywords:** metapopulation dynamics, self-persistence, network persistence, dispersal kernel, *Amphiprion clarkii*, connectivity (6/10)

**Type of article:** Letters

**Authors:**

Allison G. Dedrick<sup>a,\*1</sup> (adedrick@stanford.edu)  
Katrina A. Catalano<sup>a</sup> (kat.catalano@rutgers.edu)  
Michelle R. Stuart<sup>a</sup> (michelle.stuart@rutgers.edu)  
J. Wilson White<sup>b</sup> (will.white@oregonstate.edu)  
Humberto R. Montes, Jr.<sup>c</sup> (junmontes@vsu.edu.ph)  
Malin L. Pinsky<sup>a</sup> (malin.pinsky@rutgers.edu)

**Author affiliations:**

- a. Department of Ecology, Evolution, and Natural Resources, Rutgers University, 14 College Farm Road, New Brunswick, NJ 08901 USA;
  - b. Department of Fisheries and Wildlife, Coastal Oregon Marine Experiment Station, Oregon State University, Newport, OR 97365 USA;
  - c. Visayas State University, Pangasugan, Baybay City, 6521 Leyte, Philippines
- \* Corresponding author; e-mail: adedrick@stanford.edu  
1. Current address: Stanford Woods Institute for the Environment, Stanford University, Stanford, CA 94305 USA

**Corresponding author:**

Allison G. Dedrick  
adedrick@stanford.edu  
Phone: (510) 847-4752, Fax: (650) 725-3402  
Stanford Woods Institute for the Environment  
Jerry Yang & Akiko Yamazaki Environment & Energy Building - MC 4205  
473 Via Ortega  
Stanford, CA 94305

**Statement of authorship:** Conceptualization, Methodology: MLP, JWW, and

AGD. Investigation: MLP, MRS, KAC, and AGD. Software, Formal Analysis, Visualization: AGD. Resources: HRM. Data Curation: MRS. Writing - Original Draft: AGD. Writing - Review and Editing: AGD, KAC, MRS, JWW, HRM, MLP. Supervision, Funding Acquisition: MLP.

**Data accessibility statement:** Sample data, metadata, and analysis code are stored in a GitHub repository ([https://github.com/pinskylab/Clownfish\\_persistence](https://github.com/pinskylab/Clownfish_persistence)). The repository is public and will be archived with a DOI through Zenodo after acceptance.

**Words in the abstract:** 149/150

**Words in the main text:** 5243

**Number of references:** 66

**Number of main figures, tables, and text boxes:** 6

**Number of supplementary figures, tables, and text boxes:** 19

## Abstract

Determining metapopulation persistence requires an understanding of both demographic rates and connectivity among patches. Persistence is well understood in theory but has proved challenging to test empirically for marine and other species with high connectivity that precludes classic colonization/extinction dynamics. Here, we assessed persistence for a metapopulation of yellowtail anemonefish (*Amphiprion clarkii*) using seven years of annual sampling data along 30 km of coastline. We also carefully accounted for uncertainty in demographic rates. Despite stable population sizes through time and sufficient production of surviving offspring for replacement, the spatial pattern of connectivity made the metapopulation unlikely to persist in isolation. To persist, the metapopulation would need higher fecundity or to retain essentially all of the recruits it produced. This assessment of persistence in a marine metapopulation shows that stable abundance alone does not indicate persistence, emphasizing the necessity of assessing both demographic and connectivity processes to understand metapopulation dynamics.

# Introduction

The dynamics and persistence of metapopulations depend both on connectivity  
18 among patches and on demographic rates within each patch (Hastings and Botsford,  
2006; Hanski, 1998). For marine species, connectivity among habitat patches primarily  
occurs during planktonic larval stages when individuals are hard to track and are  
21 able to travel long distances with ocean currents. Because larval connectivity has  
been perceived to be the greatest uncertainty in these systems, research has centered  
on quantifying that component (reviewed by White et al., 2019). More recently,  
24 it has become apparent that variation in demographic rates among patches is also  
an uncertain aspect of marine metapopulation dynamics (Hameed et al., 2016; White  
and Samhouri, 2011). Given both of those uncertainties and driven by both fundamental  
27 ecological questions and applied needs (Botsford et al., 2001; White et al., 2010), a  
large body of theory has developed to describe how connectivity and local demography  
interact to determine whether marine metapopulations persist (Burgess et al., 2014;  
30 Botsford et al., 2019). Testing this theory, however, has proven substantially more  
difficult.

For any population to persist, individuals must on average replace themselves  
33 during their lifetime. Assessing replacement must account for demographic processes  
across the life cycle, including how likely individuals are to survive to the next age or  
stage, their expected fecundity at each stage, the survival to recruitment of any  
36 offspring produced, and the distribution of offspring across space (Hastings and  
Botsford, 2006). A metapopulation can persist via two mechanisms: 1) at least

one patch achieves replacement in isolation (self-persistence), or 2) multiple patches  
39 receive enough recruitment to achieve replacement through multi-generational loops  
of connectivity with other patches in the metapopulation (network persistence) (Hastings  
and Botsford, 2006; Burgess et al., 2014). Theory predicts that habitat patches that  
42 are large relative to the mean dispersal distance are likely to be self-persistent (White  
et al., 2010).

New ways of identifying individuals and determining their origins now allow better  
45 measurements of connectivity in marine populations (Almany et al., 2017; D'Aloia  
et al., 2013). Additionally, a better appreciation of the relevant theory has led  
to measurement of the demographic factors necessary to assess persistence in field  
48 metapopulations (Carson et al., 2011; Hameed et al., 2016; Johnson et al., 2018; Salles  
et al., 2015). To date, research has suggested that populations on isolated islands can  
be self-persistent, which might be expected given that they lack nearby populations  
51 from which to receive larvae (Salles et al., 2015). In contrast, small habitat patches  
spread across a larger reef metapopulation appear to rely on input from surrounding  
and intervening patches for persistence (Johnson et al., 2018). Isolated habitat  
54 patches are rare in the marine environment and clarifying whether intervening habitat  
patches are sufficient to allow metapopulations to achieve replacement is a key  
question. Persistence has yet to be quantified in the field for a continuous marine  
57 metapopulation.

Here, we further our understanding of metapopulation dynamics in a network  
of patches along a continuous coastline through a study of yellowtail anemonefish  
60 (*Amphiprion clarkii*) in the Philippines. We assessed persistence for all patches

of habitat within a metapopulation spread across 30 km of coastline. Based on seven years of data, we found that, despite containing multiple patches with large abundances that were stable over time, the metapopulation was not likely to be persistent without immigration from outside patches.

## Methods

### **66 Persistence theory and metrics**

We considered four primary metrics to assess whether and how the anemonefish metapopulation was persistent: 1) lifetime recruit production (LRP) to assess whether the metapopulation had enough offspring that survived anywhere to achieve replacement, 2) self-persistence (SP) to assess whether any individual patch could persist in isolation without input from other patches, 3) network persistence ( $\lambda_c$ ) to assess whether the metapopulation was persistent as a connected unit, and 4) local replacement (LR) to assess whether a sufficient number of recruits were retained anywhere within the metapopulation to achieve replacement, without explicitly estimating dispersal patterns (Fig. 1a-d). We explain each metric below in detail. To represent the uncertainty in our estimates, we calculated each metric 1000 times, sampling each input parameter from a distribution representing the uncertainty in the empirical estimate (details in Appendix Methods A.9 in Supporting Information). In our results, we show point estimates of each metric along with uncertainty bounds, defined as the middle 95% of the distribution of values calculated in this Monte Carlo procedure. We provide additional method details, results, tables and figures

in the appendix (methods: Appendix A, results: Appendix B, tables: Appendix C, figures: Appendix D).

<sup>84</sup> **Lifetime recruit production (LRP)**

$LRP_i$  is the expected number of recruits a recruit on patch  $i$  will produce in its lifetime,

$$LRP_i = LEP_i \times S_e, \quad (1)$$

<sup>87</sup> where  $LEP_i$  (lifetime egg production) is the patch-specific number of eggs a recruit produces in its lifetime and  $S_e$  (egg-recruit survival) is the fraction of eggs that survive to become recruits (Appendix Fig. D.1).

<sup>90</sup> If  $LRP \geq 1$ , individuals produced enough surviving offspring, before considering dispersal, to potentially achieve replacement. If  $LRP < 1$ , the population could not persist without input from outside patches. We considered all recruits produced by <sup>93</sup> adults in our metapopulation to estimate  $LRP_i$ , regardless of where they settled.

**Self-persistence (SP)**

$SP_i$  is the number of offspring a recruit produces that survive to become recruits and <sup>96</sup> settle in the natal patch,

$$SP_i = LRP_i \times p_{i,i}, \quad (2)$$

where  $p_{i,i}$  is the probability of larval retention on patch  $i$ .

A patch  $i$  is self-persistent if  $\text{SP}_i \geq 1$ . If at least one patch is self-persistent, the  
99 metapopulation as a whole persists as well (Hastings and Botsford, 2006; Burgess  
et al., 2014).

### Network persistence ( $\lambda_c$ )

102 Network persistence is the largest real eigenvalue  $\lambda_C$  of the realized connectivity  
matrix  $C$ ,

$$C_{i,j} = \text{LRP}_i \times p_{i,j}, \quad (3)$$

created by multiplying lifetime recruit production ( $\text{LRP}_i$ ) by dispersal probabilities  
105 among pairs of patches ( $p_{i,j}$ ) (Burgess et al., 2014). The diagonal entries of  $C$  are  
the self-persistence values for each patch ( $\text{SP}_i$ ).

Network persistence explicitly considers dispersal of individuals among patches  
108 in addition to the reproduction and survival at each patch and requires  $\lambda_C \geq 1$  for  
the network to persist without outside input (Hastings and Botsford, 2006; White  
et al., 2010; Burgess et al., 2014).

### 111 Local replacement (LR)

Local replacement (LR) is the number of recruits a recruit produces in its lifetime  
that return to settle within the focal metapopulation. LR is related to LRP, but in  
114 contrast, LRP also includes recruits that settle outside of the focal metapopulation.

LR is defined as

$$LR = LEP_* \times R_e, \quad (4)$$

where  $LEP_*$  is lifetime egg production averaged across patches and  $R_e$  is the proportion of eggs that survived and returned to recruit at the patches in our focal metapopulation (the 30 km section of coastline).  $R_e$  is a modification of egg-recruit survival ( $S_e$ ) that implicitly considers dispersal in terms of larvae landing inside or outside the metapopulation.

If  $LR \geq 1$ , enough offspring were locally retained to achieve replacement if they were evenly spread among patches, but the actual dispersal patterns among the metapopulation patches may still prevent replacement if the pattern of multigenerational replacement does not satisfy network persistence ( $\lambda_c$ ).  $LR$  and  $\lambda_c$  both assess the ability of our patches to persist as an isolated group, but  $LR$  treats the network as one large homogenous patch while  $\lambda_c$  explicitly accounts for the structure and connectivity among patches.

## Study species

We focused on a tropical metapopulation of yellowtail anemonefish (*Amphiprion clarkii*, Fig. 2c). Yellowtail anemonefish have a mutualistic relationship with anemones that house small colonies of fish (Buston, 2003b; Fautin et al., 1992). Yellowtail anemonefish are protandrous hermaphrodites and maintain a size-structured hierarchy; within an anemone, the largest fish is the breeding female, the next largest is the breeding male, and any smaller fish are non-breeding juveniles. The fish move up in

rank to become breeders only after the larger fish have died. In the tropical patch reef habitat of the Philippines, yellowtail anemonefish primarily spawn from November to May and lay clutches of benthic eggs that the parents protect and tend (Ochi, 1989; Holtswarth et al., 2017). Larvae hatch after about six days and spend 7–10 days in the water column before returning to reef habitat to settle in an anemone (Fautin et al., 1992).

Anemonefish are well-suited to metapopulation studies because dispersal only occurs during the larval phase and adults have limited movement on discrete habitat patches (anemones) (e.g., Buston and D'Aloia, 2013; Salles et al., 2015; Almany et al., 2017). Yellowtail anemonefish tend to behave more like other reef fishes, with wider-ranging territories and stronger swimming abilities (Hattori and Yanagisawa, 1991; Ochi, 1989) than the smaller *A. percula* commonly used in metapopulation studies (e.g., Buston et al., 2011; Salles et al., 2015).

## Field data collection

We focused on a set of nineteen reef patches spanning 30 km along the western coast of Leyte island facing the Camotes Sea in the Philippines (Fig. 2a). The habitat patches covered approximately 20% of the sampling region and consisted of rocky patches of coral reef separated by sand flats (Fig. 2a,b). To the north, the patches were isolated from nearby habitat with no substantial reef habitat for at least 20 km, a distance greater than the mean dispersal distance for this species (Pinsky et al., 2010). As such, we considered this to be a relatively isolated metapopulation. Located near a populated coastline, the region experiences anthropogenic effects

including fishing, pollution, and runoff from agriculture and a nearby riverbed gravel mine, as well as reef-destroying storms like Haiyan and other typhoons in 2013.

159     From 2012-2018, we sampled fish and habitat at most patches each year (Appendix  
Table C.4). Divers using SCUBA and tethered to GPS readers swam the extent  
of each patch and visited anemones inhabited by yellowtail anemonefish. At each  
162 anemone, the divers caught fish 3.5 cm and larger, took a tissue sample, measured  
fork length, and noted tail color as an indicator of life stage (Moyer, 1976). Starting  
in 2015, fish 6.0 cm and larger were also tagged with a passive integrated transponder  
165 (PIT) tag unless already tagged. Divers also looked for eggs around each anemone  
and measured and photographed any clutches found. In total, we took fin clips  
from and genotyped 2406 fish and PIT-tagged 1929 fish across all years and patches  
168 combined, marking 3053 individual fish.

## Estimating demographic and dispersal parameters from empirical data

### 171 Parentage analysis and dispersal kernel

Over seven years of sampling, we genotyped 1729 potential parents and 791 juveniles  
(some fish fall into both categories in different years) at 1340 single nucleotide  
174 polymorphisms (SNPs) and found 71 parent-offspring matches (Catalano et al., in  
press). We used a distance-based generalized Gaussian dispersal kernel fit from  
the parent-offspring matches (Catalano et al., in press; Bode et al., 2018), where  
177 the relative probability of dispersal  $p$  is a function of distance  $d$  in kilometers and

parameters  $\theta$  and  $K_d$  that control the shape and scale of the kernel (Fig. 3a, Appendix Table C.1, uncertainty details in Appendix Methods A.9). The dispersal kernel estimates the relative dispersal by distance for fish that have survived and recruited, so it does not separately estimate pre-settlement mortality. To find the one-tailed probability of fish dispersing among our patches, we numerically integrated the dispersal kernel using the distance from the middle of the origin patch ( $i$ ) to the closest ( $d_1$ ) and farthest ( $d_2$ ) edges of the destination patch ( $j$ ), with distances calculated using the `geosphere` package in R (Hijmans, 2017):

$$p_{i,j} = \frac{e^{K_d\theta}}{2\Gamma(\frac{1}{\theta})} \int_{d_1}^{d_2} e^{-(e^{K_d d})^\theta} dd, \quad (5)$$

where  $\Gamma$  indicates the gamma function.

### Growth and survival: mark-recapture analyses

Fish marked through genotyping and PIT tags allowed us to estimate growth and survival through mark-recapture. In total, we had 3053 marked fish with size and stage data at each capture.

For growth, we used a von Bertalanffy growth curve:

$$\begin{aligned} L_{t+1} &= L_t + (L_\infty - L_t)[1 - e^{(-k)}] \\ &= e^{(-k)}L_t + L_\infty[1 - e^{(-k)}], \end{aligned} \quad (6)$$

where  $L_\infty$  is the asymptotic maximum size across the metapopulation and  $k$  is

the growth rate. We estimated the parameters from the slope  $m$  and y-intercept  $b_L$  of the relationship between the length at first capture  $L_t$  and the length at a later  
195 capture date  $L_{t+1}$  for fish recaptured a year later (within 345 to 385 days). The von Bertalanffy parameters are  $k = -\ln(m)$  and  $L_\infty = b_L(1-m)$  (Hart and Chute, 2009)  
(Fig. 3b, Appendix Table C.1, uncertainty details in Appendix Methods A.9).

198 We used the full set of marked fish to estimate annual survival  $\phi$  and probability  
of recapture  $p_r$  using the mark-recapture program MARK implemented in R through  
the package **RMark** (Laake, 2013). We fit several models with year, size, and patch  
201 effects on the probability of survival on a log-odds scale and selected the model with  
the lowest  $AIC_c$  (Fig. 3c, details in Appendix Methods A.3, uncertainty details in  
Appendix Methods A.9, and full list of models in Appendix Table C.3).

204 **Fecundity**

From a regression of eggs per clutch on female size while accounting for egg age  
(determined by the presence of eyed eggs), we found that fecundity increased with  
207 size (Appendix eqn. A.1, see details in Appendix Methods A.4). We only considered  
reproductive effort for female fish. For sex transition size  $L_f$ , we used the average size  
at which recaptured fish were first observed as female (Fig. 3d, uncertainty details  
210 in Appendix Methods A.9).

### Lifetime egg production (LEP)

We used an integral projection model (IPM) (Ellner et al., 2016) with size as the  
213 continuous structuring trait  $L$  to estimate lifetime egg production on each patch  $i$

( $\text{LEP}_i$ ). We initialized the IPM with one recruit-sized individual (recruit defined in Appendix Methods A.1) at the initial annual time step ( $t = 0$ ), then projected forward for 100 years. We used the size- and site-dependent survival (Appendix eqn. B.1) and growth (eqn. 6) functions as the probability density functions in the kernel to project the individual into the next time step, producing a size distribution across time ( $v_{L,t}$ ). We then multiplied by size-dependent fecundity  $f_L$  (Appendix eqn. A.1). Integrating across time and size, from a minimum size  $L_s = 0$  cm to a maximum  $U_s = 15$  cm, gave us the total number of eggs one recruit produced in its lifetime (details in Appendix Methods A.5, uncertainty details in Appendix Methods A.9):

$$\text{LEP} = \int_{t=0}^{\infty} \int_{L=L_s}^{L=U_s} v_{L,t} f_L dL dt. \quad (7)$$

We calculated LEP by patch ( $\text{LEP}_i$ ) and averaged across patches ( $\text{LEP}_*$ ) for a fish of recruit size. We also calculated LEP for a fish of parent size (6.0 cm) averaged across patches ( $\text{LEP}_p$ ), which is used below to estimate egg-recruit survival.

### Accounting for density dependence

We would ideally assess persistence when the population is at low abundance and not limited by density dependence; at high density the population growth rate will slow to zero. Density dependence has not been typically addressed in previous metapopulation persistence studies (Johnson et al., 2018; Carson et al., 2011; Hameed et al., 2016), though Salles et al. (2015) considers carrying capacity and available space. Density dependence is particularly clear in anemonefish. Juveniles will

prevent others from settling such that each anemone can house only one recently  
 234 settled anemonefish (Buston, 2003a). This density-dependent mortality reduces  
 the apparent survival of new recruits from our field measurements. We accounted  
 for this effect by scaling up our estimate of recruits (the numerator of eqn. 8,  
 237 described next) by the proportional increase ( $D$ ) in unoccupied anemones if all  
 of the anemones occupied by yellowtail anemonefish were unoccupied, where  $p_A$   
 is the proportion of anemones occupied by yellowtail anemonefish and  $p_U$  is the  
 240 proportion of unoccupied anemones:  $D = \frac{(p_U + p_A)}{p_U}$ . We present results with this  
 density dependence modification in the main text and without the modification in  
 the appendix (with subscript D in Appendix Results B.8, Appendix Figs. D.9, D.10).

243 **Survival from egg to recruit ( $S_e$ )**

We estimated survival from egg to recruit ( $S_e$ ) using parentage matches to find the  
 number of surviving recruits produced by genotyped parents (similar to Johnson  
 246 et al., 2018). However, the number of offspring we assigned back to parents ( $R_m$ )  
 is an underestimate of the offspring produced by genotyped parents because it is  
 impossible to sample exhaustively. To account for unsampled offspring, we divided  
 249  $R_m$  by four factors (described below and with details in Appendix Methods A.8 and  
 Appendix Fig. D.2), in addition to multiplying by  $D$  as described above, then divided  
 by the number of eggs produced by genotyped parents:

$$S_e = \frac{\frac{DR_m}{P_h P_c P_d P_s}}{N_g \text{LEPp}}, \quad (8)$$

252 where  $N_g$  was the number of genotyped parents and LEPp was the expected  
 lifetime egg production for a fish that has already survived to parent size p (=6.0cm).  
 255  $P_h$  was the cumulative proportion of habitat in our patches that we sampled over  
 time,  $P_c$  was the probability of capturing a fish if we sampled its anemone,  $P_d$  was  
 the proportion of the total dispersal kernel from each of our patches covered by  
 our sampling region, and  $P_s$  was the proportion of suitable habitat in our sampling  
 258 region (details in for each in Appendix Methods A.8, uncertainty of  $P_c$  in Appendix  
 Methods A.9).

To estimate the survival and retention of recruits back to our patches (needed for  
 261 local replacement, LR, eqn. 4), we scaled only by  $P_h$  and  $P_c$ :

$$R_e = \frac{\frac{DR_m}{P_h P_c}}{N_g \text{LEPP}}. \quad (9)$$

## Estimated abundance over time

We examined trends in abundance of breeding females at each patch over time ( $F_{i,t}$ )  
 264 to compare to our replacement-based persistence estimates. As with offspring, we  
 scaled up the number of females caught ( $F_{c_{i,t}}$ ) at each patch  $i$  in each sampling year  
 267  $t$  by the proportion of habitat sampled in that patch and year ( $P_{h_{i,t}}$ ) and by the  
 probability of capturing a fish  $P_c$ :

$$F_{i,t} = \frac{F_{c_{i,t}}}{P_{h_{i,t}} P_c} \quad (10)$$

We fit a mixed effects model with Poisson errors in which  $F_{i,t}$  was the response

variable, year was the fixed effect, and there were random effects by patch for both  
270 intercept and slope using the package `lme4` in R (Bates et al., 2015).

## Exploring alternative geographies and larval navigation

To understand whether results would likely be similar in other geographies, we tested  
273 the sensitivity of metapopulation persistence to alternative patch widths and to the  
proportion of the region that is habitat. We varied the proportion of habitat and the  
overall width of the region using 19 equally sized and spaced patches. We created  
276 connectivity matrices using the new distances between patches and otherwise used  
the original parameter values and uncertainty sets, using adult survival ( $\phi$ ) from the  
patch with median survival (the Elementary School patch) for all patches.

279 We also tested sensitivity to the ability of larvae to navigate to habitat by adding  
up to a 1 km buffer to the edges of the destination patches when integrating the  
dispersal kernel and adjusting the scaling parameter  $P_s$  (eqn. 8) to account for fewer  
282 larvae being lost between patches (details in Appendix Methods A.7).

# Results

## Demographic rates

285 From field data, mark-recapture, and parentage analyses, we estimated growth (Fig.  
3b, Appendix Results B.3), fecundity (Appendix Table C.1), annual survival (Fig.  
3c, Appendix Fig. D.5, Appendix Results B.4), lifetime egg production (Fig. 4a,  
288 Appendix Results B.6), egg-recruit survival (Appendix Fig. D.13, Appendix Results

B.7), and the dispersal kernel (Fig. 3a, Appendix Results B.2). Details and estimated values are in the Results (Appendix B) and Tables (Appendix C) sections of the  
291 appendix. These demographic rates form the basis for assessing whether and how the metapopulation persists.

## Persistence metrics

294 Using our demographic and dispersal results, we estimated average lifetime recruit production (LRP) across patches to be 1.74 [0.93, 5.55] (Fig. 4b, Appendix Fig. D.12). Best estimates of  $LRP_i$  at individual patches ranged from 0 to 3.7 (Appendix  
297 Table C.5, Appendix Fig. D.8). Averaged across patches, 95% of LRP estimates were  $\geq 1$ , which means that individuals produced enough offspring to replace themselves. However, LRP does not tell us whether those offspring settled in locations that  
300 contributed to persistence.

Considering retention of larvae at individual patches, we did not find any patches with  $SP_i \geq 1$  (Fig. 5a), suggesting that no patch could persist in isolation. The  
303 Haina patch came closest to self-persistence ( $SP_i = 0.088$  [0.009, 0.47]) and had only 0.5% of uncertainty values  $\geq 1$ , making self-persistence very unlikely.

For network persistence, our estimate of  $\lambda_c$  was 0.20 [0.11, 0.84], with only 1.2%  
306 of the estimates of  $\lambda_c \geq 1$  (Fig. 5c, Appendix Fig. D.14). Network persistence for this metapopulation was therefore highly unlikely but not impossible. Our estimate of local replacement (LR) was 0.20 [0.11, 0.63], also suggesting lack of independent  
309 persistence of this group of patches and very similar to our  $\lambda_c$  estimate. While both LR and  $\lambda_c$  provide information on the ability of our patches to persist as an

isolated group, they differ in their assumption of the structure of the population. LR  
312 approximates the network of patches as a single well-mixed unit, while  $\lambda_c$  incorporates  
the spatial structure of the patches and multi-generation dynamics. Results without  
density dependence compensation also suggested lack of persistence (Appendix Results  
315 B.8, Appendix Fig. D.9).

## Abundance

Our estimated abundance of females over time had a positive trend for the average  
318 patch (slope = 1.08, Fig. 4d), suggesting a slight increase in population size through  
time. Most individual patches also showed a positive trend in female abundance  
through time (Fig. 4d, Appendix Fig. D.7). Therefore, though the metapopulation  
321 did not exhibit network persistence, it also did not show signs of decline over the  
time scale of our study.

## Alternative production and geographies

324 We then examined what conditions would be needed for this metapopulation to reach  
persistence. With the existing patch configuration and dispersal kernel, the system  
would need  $LRP \geq 8.4$  (a five-fold increase) to reach network persistence. In turn,  
327 this would require a five-fold increase of egg-recruit survival ( $S_e$ ), or  $LEP_*$ , or an  
equivalent combination of increases across both. If we alternatively considered all  
arriving recruits as offspring (not just those originating within the metapopulation),  
330  $LRP$  would be 11.1, which would be sufficient for persistence. Similarly, our estimate  
of  $LR$  using all recruits arriving to the patches gave an estimate  $> 1$  (2.21), also

suggesting there was recruit-recruit replacement for the metapopulation when immigrants  
333 were included.

Another route to persistence would be with a different dispersal matrix or habitat density. If dispersal was such that the metapopulation retained all offspring produced,  
336 the study region would be persistent because  $LRP > 1$ . With the observed dispersal, however, retaining all recruits is difficult to achieve. The coastline had a low fraction  
339 of habitat (20%) and would need to be increased to about 85% before enough offspring are retained that the point estimate of  $\lambda_c \geq 1$  (Fig. 6a). In contrast, widening the region while maintaining the same habitat density (20%) did not achieve persistence (Fig. 6b) unless habitat density was also increased (Fig. 6c). As the region widens,  
342 the habitat density necessary for persistence decreases, down to 68% habitat at a region 55 km wide. In contrast, allowing for larval navigation had little impact on persistence estimates (Fig. 6d).

## 345 Discussion

In this first assessment of demographic persistence of a coastal marine metapopulation, we did not find strong evidence for either self-persistence of an individual patch or  
348 network persistence of the entire 30 km area as an isolated region. This inability to persist as an isolated region does not mean that the metapopulation was declining, however. Both population trends and replacement of recruits with immigrants showed  
351 that population levels were stable or increasing slightly. Taken together, these metrics suggest that the region required input of immigrants to persist. Despite encompassing a distance substantially larger than mean dispersal, the coastline only

<sup>354</sup> persisted as part of a larger metapopulation.

Theory for predicting persistence within patchy habitats has suggested that we expect self-persistence when the mean dispersal distance is small relative to patch size and network persistence in groups of patches when dispersal distances are much larger than patch sizes and where the proportion of habitat in the landscape is about 10-40% (depending on the particular species, population, and maximum reproductive rate, Botsford et al., 2019). Individual patches in the focal metapopulation were too small for self-persistence, but the 30 km region we sampled was about triple the mean dispersal distance of yellowtail anemonefish estimated from previous genetic work (8-9 km, Pinsky et al., 2010; Catalano et al., in press). Rather than a continuous patch, however, the region was only about 20% habitat. Increasing the proportion of habitat, however, suggested that even 40% habitat coverage would not be sufficient to achieve persistence and this metapopulation would require almost continuous habitat to persist. Similar to fish on small patches in the Caribbean (Johnson et al., 2018), this anemonefish metapopulation depends on the production and connectivity of outside patches. One possible path to persistence would be through nearby patches with higher egg production or survival. In such a case, even a small increase in area could create a persistent network. Deeper reefs, for example, are often healthier than shallower reefs (Cinner et al., 2016). In this system, offshore reefs, with higher coral cover and less silt, could have higher anemonefish survival and contribute disproportionately to regional metapopulation persistence.

<sup>375</sup> Our finding of a lack of isolated persistence differs markedly from persistence findings of other reef fish metapopulations. On reefs surrounding Kimbe Island,

Salles et al. (2015) report self-persistence of individual anemonefish subpopulations  
378 in lagoons that were of similar size (approximately 100-500 m long) to our individual  
patches, as well as network persistence of the 800 m wide metapopulation around the  
island. This persistence finding is at a dramatically smaller scale than for our focal  
381 metapopulation in the Philippines. Additionally, Johnson et al. (2018) estimated that  
four reefs of a combined area of only 2.6 km<sup>2</sup> (four 65 ha patches) would be sufficient  
for network persistence of a damselfish metapopulation across multiple islands in  
384 the Bahamas. This area is roughly equivalent to a 26 km coastline section, which  
is shorter than our sampling region. To persist, these two offshore metapopulations  
either had much higher retention of recruits or higher recruit production than did  
387 our coastline patches.

Though lack of sufficient connectivity and retention is thought to inhibit network  
persistence in some systems (e.g., insufficient retention of offspring within reserves  
390 for eastern oysters (*Crassostrea virginica*) in North Carolina; Puckett and Eggleston,  
2016), low production of surviving recruits seems the likelier explanation in the  
Philippines. Recruit production was much lower in the Philippines than in the  
393 Kimbe Island populations, where Salles et al. (2020) estimated that an average  
individual produced 0.54 offspring over two years that recruited back to the natal  
population, more than twice our estimate of lifetime local replacement (LR = 0.20).  
396 Lower production at our patches could be due to lower egg production, slower  
growth, or lower adult survival, all likely affected by habitat quality (e.g. Salles  
et al., 2020; Hayashi et al., 2019). Our study system was near a populated coastline  
399 and experienced anthropogenic effects, including pollution and silt, that can reduce

demographic rates. Adult survival, for example, was lower at the two patches just downstream of a gravel mine (N. and S. Magbangon). Even at our higher-survival  
402 patches (38% annual survival for a 6 cm fish and 53% for a 10 cm fish at Tomakin  
Dako, for example), survival was lower than estimates from the populations at  
Kimbe Island (85% annual survival, Salles et al., 2015). Estimates of annual survival  
405 in other reef fish species are closer to the lower survival we found for yellowtail  
anemonefish than the higher survival of *A. percula* at Kimbe Island (approximately  
30% annual survival for bluehead wrasse (*Thalassoma bifasciatum*) and bicolour  
408 damselfish (*Stegastes partitus*), respectively; Warner and Hughes, 1988; Figueira  
et al., 2008). Metapopulation growth rates in other reef fish (e.g., Figueira, 2009)  
and marine species more broadly (Carson et al., 2011) are highly sensitive to adult  
411 survival and other demographic parameters.

Temporal variability in demographic or dispersal parameters on a time scale  
longer than our sampling might also enable persistence of our patches in isolation  
414 (similar to the storage effect, Warner and Chesson, 1985) rather than as part of  
a larger metapopulation. Successful recruitment events on the decadal scale, for  
example, sustain rockfish populations on the west coast of the United States through  
417 the intervening weak recruitment years (e.g. Tolimieri and Levin, 2005). Our study  
could have missed a particularly strong recruitment event driven by variable ocean  
connectivity (simulations suggest that 20 years are necessary to capture the full  
420 extent of ocean variability in the Coral Triangle region surrounding our patches;  
Thompson et al., 2018). Strong recruitment would need to occur at least once a  
generation to maintain patch populations without switching to colonization and

423 extinction dynamics, however, which we do not see. Our study likely spans the generation time of a yellowtail anemonefish (roughly 5 years) so variable strong recruitment, while possible, is unlikely to sustain our populations.

426 Understanding marine population persistence in the context of broader metapopulation theory requires reconciling replacement-based persistence analysis with classic colonization-extinction and source-sink dynamics (Sale et al., 2006). At the patch level, many marine  
429 metapopulations do not exhibit the colonization-extinction dynamics (or do only on a decades to centuries timescale, Smedbol et al., 2002) that underpin our understanding of many terrestrial metapopulations (e.g, Hanski, 1998; Moilanen et al., 1998). Marine  
432 metapopulations more often instead consist of continuously-occupied patches connected by dispersal (Kritzer and Sale, 2006). Because dispersal is so widespread, patches in marine systems are not easily classified as sources or sinks in the classical fashion  
435 (Figueira and Crowder, 2006; White and Samhouri, 2011). For example, despite being unable to persist in isolation, our region is not technically a sink (Pulliam, 1988) because  $LRP > 1$ . For metapopulations, lack of self-persistence can have two causes: reproduction does not balance mortality losses within a patch (a sink) or sufficient recruits are produced but not retained (as we found in the Philippines). Metapopulations likely lie on a continuum between extinction-colonization dynamics  
438 and exchange among populated patches (Kritzer and Sale, 2006) but the latter may be a more practical approach to characterizing dynamics for metapopulations in which exchange is frequent relative to organisms' generations times (Hastings and  
441 Botsford, 2006).

In this system and others, density dependence presents a sampling challenge.

Persistence criteria (Hastings and Botsford, 2006; Burgess et al., 2014) ask whether  
447 a population at low abundance can grow and recover rather than going extinct.  
In real populations, however, it can be challenging to estimate density-independent  
demographic rates because density dependence is occurring in the population as it is  
450 sampled during dispersal (Nowicki and Vrabec, 2011) and reproduction (Rodenhouse  
et al., 2003). In anemonefish, density dependence is likely most important immediately  
post-settlement, as it is for many species, including corals, trees, and butterflies  
453 (Vermeij and Sandin, 2008; Harms et al., 2000; Nowicki et al., 2009). However,  
density dependence could continue to be important throughout life due to social  
hierarchies in anemonefish colonies (Buston and Elith, 2011). Our calculations of  
456 persistence in this paper did not account for longer term post-settlement density  
dependence, which would be an interesting area of further research.

Understanding persistence is critical for the management of spatial populations,  
459 such as siting marine protected areas (Kaplan et al., 2009), assessing habitat fragmentation  
risks (Smith and Hellmann, 2002; Fahrig, 2001) and conserving species in the face  
of climate change (Coleman et al., 2017; Fuller et al., 2015). Though models and  
462 theory provide us with expectations, we are only beginning to tackle these questions  
empirically. While rules of thumb have been widely used in marine ecology and  
conservation, they may be far from accurate for many study systems. Fortunately,  
465 tools now exist to permit a more precise evaluation of demographic rates that can  
enable assessment of persistence — or lack thereof. Spatial scales of metapopulation  
persistence in marine systems are likely to be large, despite evidence that dispersal  
468 distances are shorter than previously expected (Jones et al., 1999; Almany et al.,

2007). Importantly, persistence of coastal metapopulations may rely on high quality habitat refugia to a greater extent than has been widely recognized.

<sup>471</sup> **Acknowledgements**

We thank Visayas State University for providing scientific and logistical support during our field sampling in Leyte, Philippines, as well as the municipalities of Bay <sup>474</sup> Bay City and Albuera. We particularly thank Geralde Sucano, Jennifer Hoey, Patrick Flanagan, Joyce Ong, Apollo Lizano, Cecil Bantiles, Rodney Silvado, Beverlito Montalban, Teresita Idara, Rogello Nicanor, Liza Espinosa, Shem San Jose, Noel <sup>477</sup> Alquino, Carlos Balansuna, Froilan Beas, Danilo Marine, Tony Nahacky, and Arturo Bastasa. For financial support, we thank Rutgers School of Environmental and Biological Sciences, NSF #OCE-1430218, an Alfred P. Sloan Research Fellowship, <sup>480</sup> and an ORAU Ralph E. Powe Junior Faculty Enhancement award. This is publication number ## of PISCO, the Partnership for Interdisciplinary Study of Coastal Oceans, funded primarily by the David and Lucile Packard Foundation.

## <sup>483</sup> References

- Almany, G. R., S. Planes, S. R. Thorrold, M. L. Berumen, M. Bode, P. Saenz-Agudelo, et al. (2017). Larval fish dispersal in a coral-reef seascapes. *Nat. Ecol. Evol.*, 1:0148.
- Almany, G. R., M. L. Berumen, S. R. Thorrold, S. Planes, and G. P. Jones. (2007). Local replenishment of coral reef fish populations in a marine reserve. *Science*, 316 (5825):742–744.
- Arvedlund, M., M. I. McCormick, D. G. Fautin, and M. Bildsøe. (1999). Host recognition and possible imprinting in the anemonefish *Amphiprion melanopus* (Pisces: Pomacentridae). *Mar. Ecol. Prog. Ser.*, 188:207–218.
- Bates, D., M. Mächler, B. Bolker, and S. Walker. (2015). Fitting linear mixed-effects models using lme4. *J. Stat. Softw.*, 67(1):1–48.
- Bellwood, D. R. and R. Fisher. (2001). Relative swimming speeds in reef fish larvae. *Mar. Ecol. Prog. Ser.*, 211:299–303.
- Bode, M., D. H. Williamson, H. B. Harrison, N. Outram, and G. P. Jones. (2018). Estimating dispersal kernels using genetic parentage data. *Methods Ecol. Evol.*, 9 (3):490–501.
- Botsford, L. W., A. Hastings, and S. D. Gaines. (2001). Dependence of sustainability on the configuration of marine reserves and larval dispersal distance. *Ecol. Lett.*, 4:144–150.

- Botsford, L. W., J. W. White, and A. Hastings. (2019). *Population Dynamics for Conservation*. Oxford University Press.
- 504 Brewer, C. A. (2020). <http://www.ColorBrewer.org>, accessed 18 August 2020.
- Burgess, S. C., K. J. Nickols, C. D. Griesemer, L. A. K. Barnett, A. G. Dedrick,  
507 E. V. Satterthwaite, et al. (2014). Beyond connectivity: how empirical methods can quantify population persistence to improve marine protected-area design. *Ecol. Appl.*, 24(2):257–270.
- 510 Buston, P. (2003a). Forcible eviction and prevention of recruitment in the clown anemonefish. *Behav. Ecol.*, 14(4):576–582.
- Buston, P. (2003b). Social hierarchies: size and growth modification in clownfish.  
513 *Nature*, 424(6945):145–146.
- Buston, P. M. and C. C. D'Aloia. (2013). Marine ecology: reaping the benefits of local dispersal. *Curr. Biol.*, 23(9):R351–R353.
- 516 Buston, P. M. and J. Elith. (2011). Determinants of reproductive success in dominant pairs of clownfish: a boosted regression tree analysis. *J. Anim. Ecol.*, 80(3): 528–538.
- 519 Buston, P. M., G. P. Jones, S. Planes, and S. R. Thorrold. (2011). Probability of successful larval dispersal declines fivefold over 1 km in a coral reef fish. *Proc. Royal Soc. B.*, rspb20112041.

- 522 Carson, H. S., G. S. Cook, P. C. López-Duarte, and L. A. Levin. (2011). Evaluating  
the importance of demographic connectivity in a marine metapopulation. *Ecology*,  
92(10):1972–1984.
- 525 Catalano, K. A., A. G. Dedrick, M. R. Stuart, J. Purtiz, H. R. Montes, Jr., and  
M. L. Pinsky. (in press). Quantifying dispersal variability among nearshore marine  
populations. *Mol. Ecol.*.
- 528 Cinner, J. E., C. Huchery, M. A. MacNeil, N. A. J. Graham, T. R. McClanahan,  
J. Maina, et al. (2016). Bright spots among the worlds coral reefs. *Nature*, 535  
(7612):416–419.
- 531 Coleman, M. A., P. Cetina-Heredia, M. Roughan, M. Feng, E. Sebille, and B. P.  
Kelaher. (2017). Anticipating changes to future connectivity within a network of  
marine protected areas. *Glob. Change Biol.*, 23(9):3533–3542.
- 534 D'Aloia, C. C., S. M. Bogdanowicz, J. E. Majoris, R. G. Harrison, and P. M. Buston.  
(2013). Self-recruitment in a Caribbean reef fish: a method for approximating  
dispersal kernels accounting for seascape. *Mol. Ecol.*, 22(9):2563–2572.
- 537 Elliott, J. K., J.M. Elliott, and R.N. Mariscal. (1995). Host selection, location, and  
association behaviors of anemonefishes in field settlement experiments. *Mar. Biol.*,  
122(3):377–389.
- 540 Ellner, S. P., D. Z. Childs, and M. Rees. (2016). Data-driven modelling of structured  
populations. *A practical guide to the Integral Projection Model*. Springer.

- Fahrig, L. (2001). How much habitat is enough? *Biol. Conserv.*, 100(1):65–74.
- 543 Fautin, D. G. and G. R. Allen. (1992). Field guide to anemonefishes and their host  
sea anemones. Western Australian Museum.
- Figueira, W. F. (2009). Connectivity or demography: defining sources and sinks in  
546 coral reef fish metapopulations. *Ecol. Modell.*, 220(8):1126–1137.
- Figueira, W. F. and L. B. Crowder. (2006). Defining patch contribution in source-sink  
metapopulations: the importance of including dispersal and its relevance to marine  
549 systems. *Popul. Ecol.*, 48(3):215–224.
- Figueira, W. F., S. J. Lyman, L. B. Crowder, and G. Rilov. (2008). Small-scale  
demographic variability of the bicolor damselfish, *Stegastes partitus*, in the Florida  
552 Keys, USA. *Environ. Biol. Fishes*, 81(3):297–311.
- Fisher, R. (2005). Swimming speeds of larval coral reef fishes: impacts on  
self-recruitment and dispersal. *Mar. Ecol. Prog. Ser.*, 285:223–232.
- 555 Fuller, E., E. Brush, and M. L. Pinsky. (2015). The persistence of populations facing  
climate shifts and harvest. *Ecosphere*, 6(9):1–16.
- Hameed, S. O., J. W. White, S. H. Miller, K. J. Nickols, and S. G. Morgan.  
558 (2016). Inverse approach to estimating larval dispersal reveals limited population  
connectivity along 700 km of wave-swept open coast. *Proc. Royal Soc. B.*, 283  
(1833):20160370.
- 561 Hanski, I. (1998). Metapopulation dynamics. *Nature*, 396(6706):41–49.

- Harms, K. E., S. J. Wright, O. Calderón, A. Hernandez, and E. A. Herre. (2000). Pervasive density-dependent recruitment enhances seedling diversity in a tropical forest. *Nature*, 404(6777):493–495.
- 564
- Hart, D. R. and A. S. Chute. (2009). Estimating von Bertalanffy growth parameters from growth increment data using a linear mixed-effects model, with an application to the sea scallop *Placopecten magellanicus*. *ICES J. Mar. Sci.*, 66(10):2165–2175.
- 567
- Hastings, A. and L. W. Botsford. (2006). Persistence of spatial populations depends on returning home. *Proc. Nat. Acad. Sci.*, 103:6067–6072.
- 570 Hattori, A. and Y. Yanagisawa. (1991). Life-history pathways in relation to gonadal sex differentiation in the anemonefish, *Amphiprion clarkii*, in temperate waters of Japan. *Environ. Biol. Fishes*, 31(2):139–155.
- 573 Hayashi, K., K. Tachihara, and J. D. Reimer. (2019). Low density populations of anemonefish with low replenishment rates on a reef edge with anthropogenic impacts. *Enviro. Biol. Fishes*, 102(1):41–54.
- 576 Hijmans, R. J. (2017). *geosphere: Spherical Trigonometry*. R package version 1.5-7.
- Holtswarth, J. N., S. B. San Jose, H. R. Montes Jr., J. W. Morley, and M. L Pinsky. (2017). The reproductive seasonality and fecundity of yellowtail clownfish (*Amphiprion clarkii*) in the Philippines. *Bull. Mar. Sci.*, 93.
- 579
- Johnson, D. W., M. R. Christie, T. J. Pusack, C. D. Stallings, and M. A. Hixon.

(2018). Integrating larval connectivity with local demography reveals regional

582 dynamics of a marine metapopulation. *Ecology*, 99(6):1419–1429.

Jones, G. P., M. J. Milicich, M. J. Emslie, and C. Lunow. (1999). Self-recruitment  
in a coral reef fish population. *Nature*, 402(6763):802–804.

585 Kaplan, D. M., L. W. Botsford, M. R. O'Farrell, S. D. Gaines, and S. Jorgensen.  
(2009). Model-based assessment of persistence in proposed marine protected area  
designs. *Ecol. Appl.*, 19(2):433–448.

588 Kritzer, J. P. and P. F. Sale. (2006). *Marine Metapopulations*. Elsevier Academic  
Press.

Laake, J. L. (2013). RMark: An R interface for analysis of capture-recapture data  
591 with MARK. R package version 2.2.6.

Lecchini, D., S. Planes, and R. Galzin. (2005). Experimental assessment of sensory  
modalities of coral-reef fish larvae in the recognition of their settlement habitat.  
594 *Behav. Ecol. Sociobiol.*, 58(1):18–26.

Moilanen, A., A. T. Smith, and I. Hanski. (1998). Long-term dynamics in a  
metapopulation of the American pika. *Am. Nat.*, 152(4):530–542.

597 Moyer, J. T. (1976). Geographical variation and social dominance in Japanese  
populations of the anemonefish *Amphiprion clarkii*. *Jpn. J. Ichthyol.*, 23(1):12–22.

Nowicki, P. and V. Vrabec. (2011). Evidence for positive density-dependent  
600 emigration in butterfly metapopulations. *Oecologia*, 167(3):657.

- Nowicki, P., S. Bonelli, F. Barbero, and E. Balletto. (2009). Relative importance of density-dependent regulation and environmental stochasticity for butterfly population dynamics. *Oecologia*, 161(2):227–239.
- Ochi, H. (1989). Mating behavior and sex change of the anemonefish, *Amphiprion clarkii*, in the temperate waters of southern Japan. *Environ. Biol. Fishes*, 26(4): 257–275.
- Pinsky, M. L., H. R. Montes Jr, and S. R. Palumbi. (2010). Using isolation by distance and effective density to estimate dispersal scales in anemonefish. *Evolution*, 64(9): 2688–2700.
- Puckett, B. J. and D. B. Eggleston. (2016). Metapopulation dynamics guide marine reserve design: importance of connectivity, demographics, and stock enhancement. *Ecosphere*, 7(6).
- Pulliam, H. R. (1988). Sources, sinks, and population regulation. *Am. Nat.*, 132(5): 652–661.
- Rodenhouse, N. L., T. S. Sillett, P. J. Doran, and R. T. Holmes. (2003). Multiple density-dependence mechanisms regulate a migratory bird population during the breeding season. *Proc. Royal Soc. B.*, 270(1529):2105–2110.
- Sale, P. F., I. Hanski, and J. P. Kritzer. (2006). The merging of metapopulation theory and marine ecology: establishing the historical context. In *Marine Metapopulations*, pp. 3–28. Elsevier.

- 621 Salles, O. C., G. R. Almany, M. L. Berumen, G. P. Jones, P. Saenz-Agudelo, M.  
Srinivasan, et al. (2020). Strong habitat and weak genetic effects shape the lifetime  
reproductive success in a wild clownfish population. *Ecol. Lett.*, 23(2):265–273.
- 624 Salles, O. C., J. A. Maynard, M. Joannides, C. M. Barbu, P. Saenz-Agudelo, G. R.  
Almany, et al. (2015). Coral reef fish populations can persist without immigration.  
*Proc. Royal Soc. B.*, 282(1819):20151311.
- 627 Smedbol, R. K., A. McPherson, M. M. Hansen, and E. Kenchington. (2002). Myths  
and moderation in marine metapopulations? *Fish Fish. (Oxf)*, 3(1):20–35.
- Smith, J. N. M. and J. J. Hellmann. (2002). Population persistence in fragmented  
landscapes. *Trends Ecol. Evol.*, 17(9):397–399.
- 630 Thompson, D. M., J. Kleypas, F. Castruccio, E. N. Curchitser, M. L. Pinsky,  
B. Jönsson, et al. (2018). Variability in oceanographic barriers to coral larval  
dispersal: Do currents shape biodiversity? *Prog. Oceanogr.*, 165:110–122.
- Tolimieri, N. and P. S. Levin. (2005). The roles of fishing and climate in the  
population dynamics of bocaccio rockfish. *Ecol. Appl.*, 15(2):458–468.
- 636 Vermeij, M. J. A. and S. A. Sandin. (2008). Density-dependent settlement and  
mortality structure the earliest life phases of a coral population. *Ecology*, 89(7):  
1994–2004.
- 639 Warner, R. R. and P. L. Chesson. (1985). Coexistence mediated by recruitment  
fluctuations: a field guide to the storage effect. *Am. Nat.*, 125(6):769–787.

- Warner, R. R. and T. P. Hughes. (1988). The population dynamics of reef fishes.  
642 6th International Coral Reef Symposium Executive Committee.
- White, J. W. and J. F. Samhouri. (2011). Oceanographic coupling across three  
trophic levels shapes source–sink dynamics in marine metacommunities. *Oikos*,  
645 120(8):1151–1164.
- White, J. W., M. H. Carr, J. E. Caselle, L. Washburn, C. B. Woodson, S. R.  
Palumbi, et al. (2019). Connectivity, dispersal, and recruitment: Connecting  
648 benthic communities and the coastal ocean. *Oceanography*, 32(3):50–59.
- White, J. W., L. W. Botsford, A. Hastings, and J. L. Largier. (2010). Population  
persistence in marine reserve networks: incorporating spatial heterogeneities in  
651 larval dispersal. *Mar. Ecol. Prog. Ser.*, 398:49–67.

# Figures

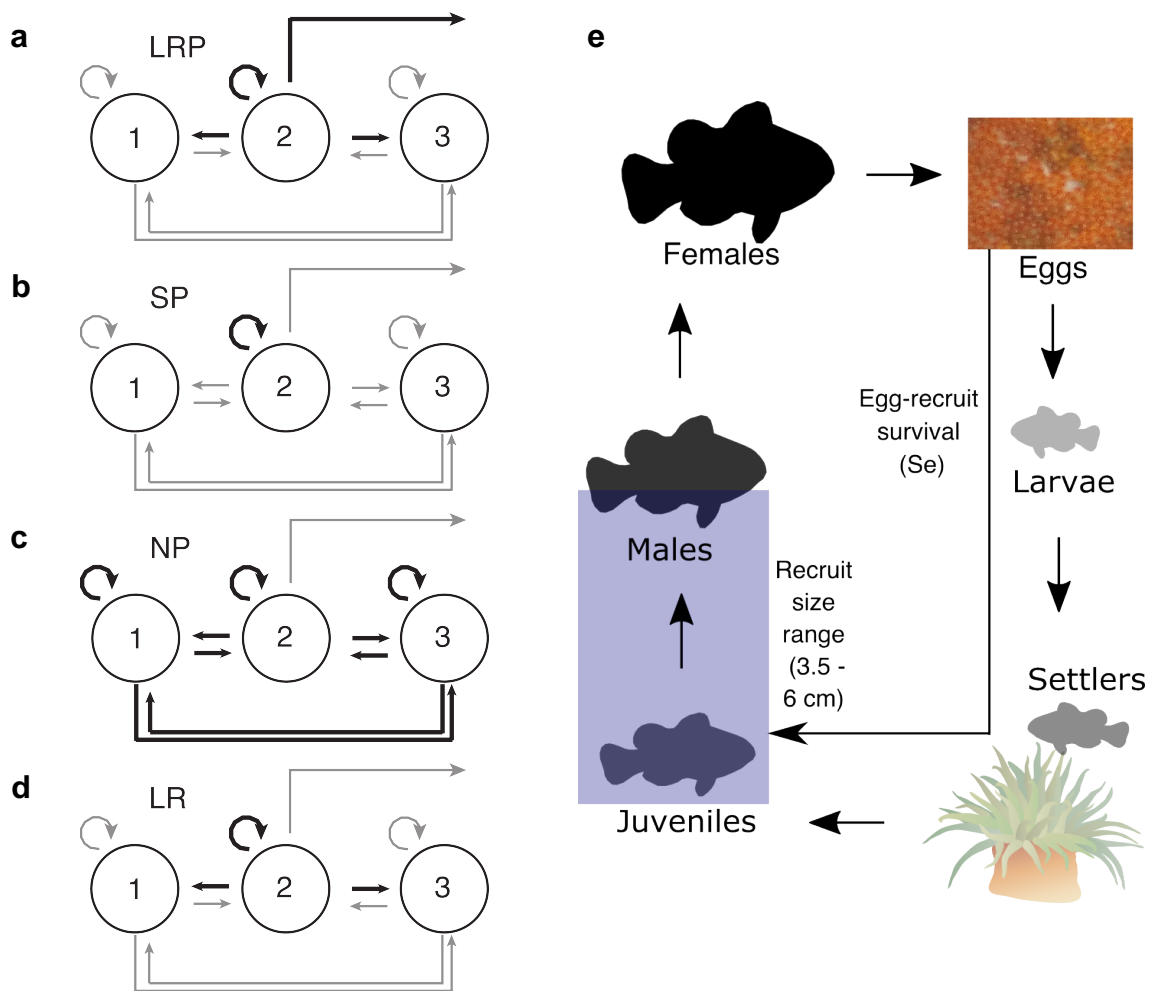


Figure 1: Schematics of the persistence metrics (a-d): a) lifetime recruit production (LRP, eqn. 1), b) self-persistence (SP, eqn. 2), c) network persistence ( $\lambda_c$ , first eigenvalue of eqn. 3), and d) local replacement (LR, eqn. 4). Black lines indicate the demographic processes considered by each persistence metric. e) The life cycle of yellowtail anemonefish, including the range of sizes considered to be recruits (recruit definition in Appendix Methods A.1).

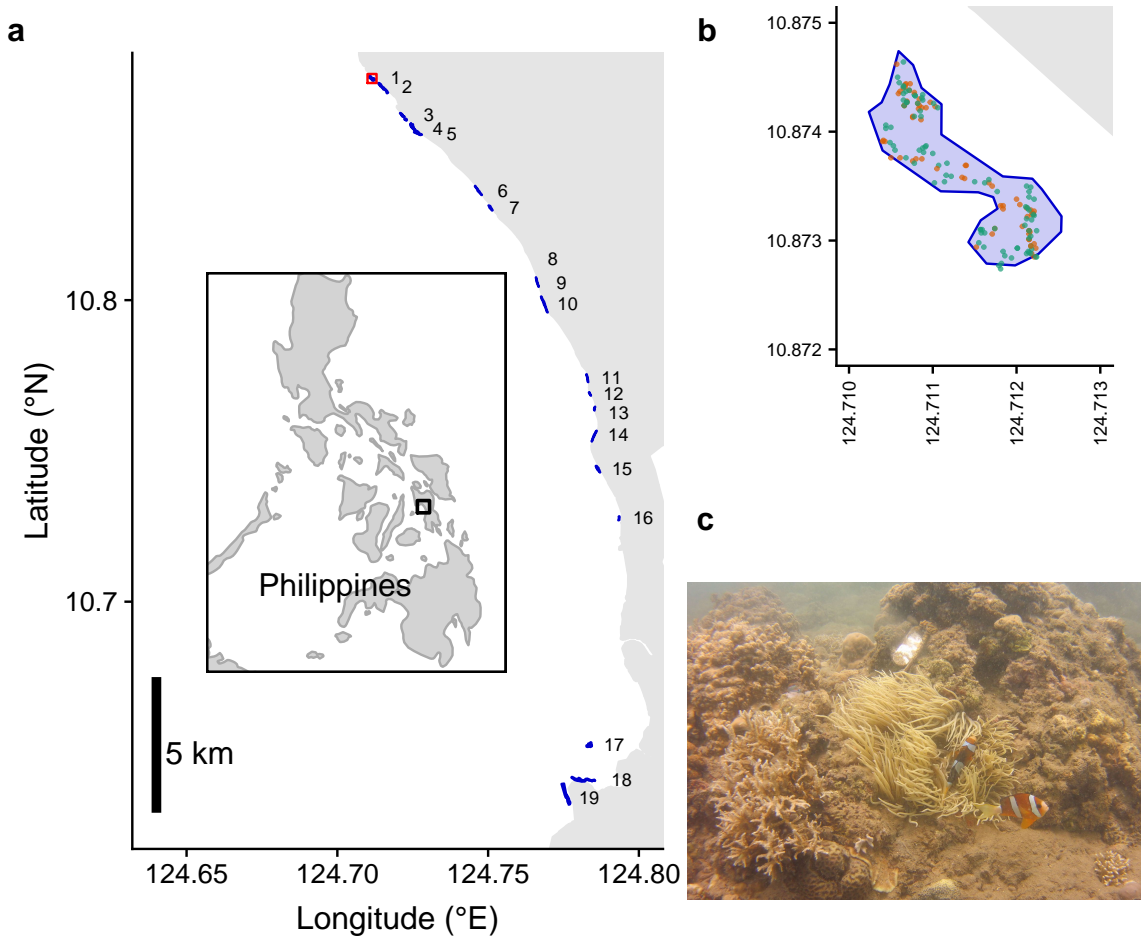


Figure 2: a) Map of the patches along the coast of Leyte in the Philippines. From north to south, the patches are: 1) Palanas, 2) Wangag, 3) North Magbangon, 4) South Magbangon, 5) Cabatoan, 6) Caridad Cemetery, 7) Caridad Proper, 8) Hicop South, 9) Sitio Tugas, 10) Elementary School, 11) Sitio Lonas, 12) San Agustin, 13) Poroc San Flower, 14) Poroc Rose, 15) Visca, 16) Gabas, 17) Tomakin Dako, 18) Haina, and 19) Sitio Baybayon. b) Zoomed-in map of the northern-most patch, Palanas (red box on map), to show anemone arrangement. Anemones are colored as occupied by yellowtail anemonefish (green) or unoccupied by anemonefish (orange), using colors generated with Brewer (2020). c) An example anemone occupied by yellowtail anemonefish in a typical habitat. The metal anemone tag is visible just above the anemone on the rock.

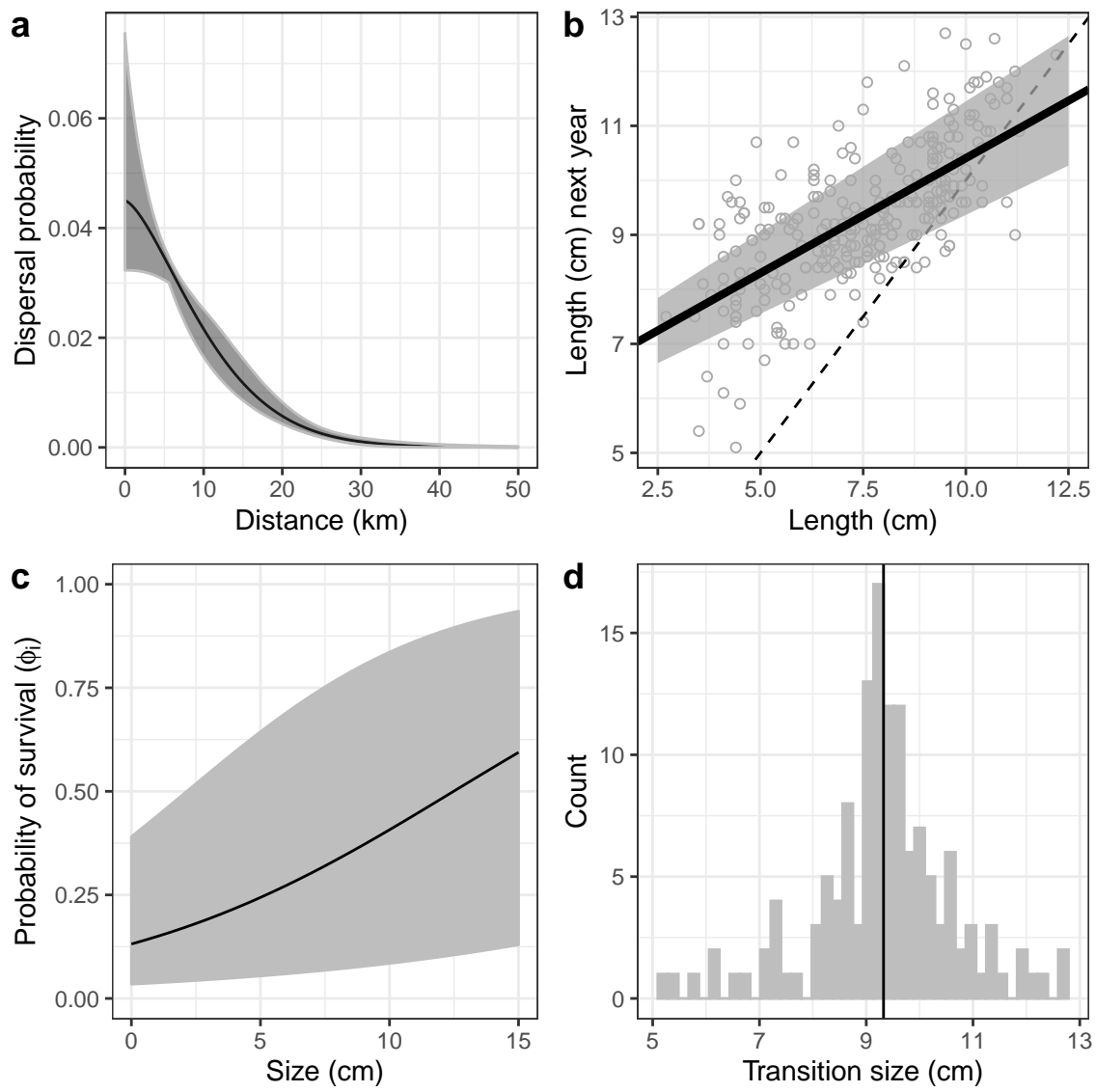


Figure 3: Estimates (solid black line) and uncertainty (grey) for a) dispersal (eqn. 5), b) growth (eqn. 6), including a dashed 1:1 line, c) post-recruit annual survival (Appendix eqn. B.1) at the example patch Elementary School, and d) raw data of fish size at female transition ( $L_f$  in Appendix eqn. A.1).

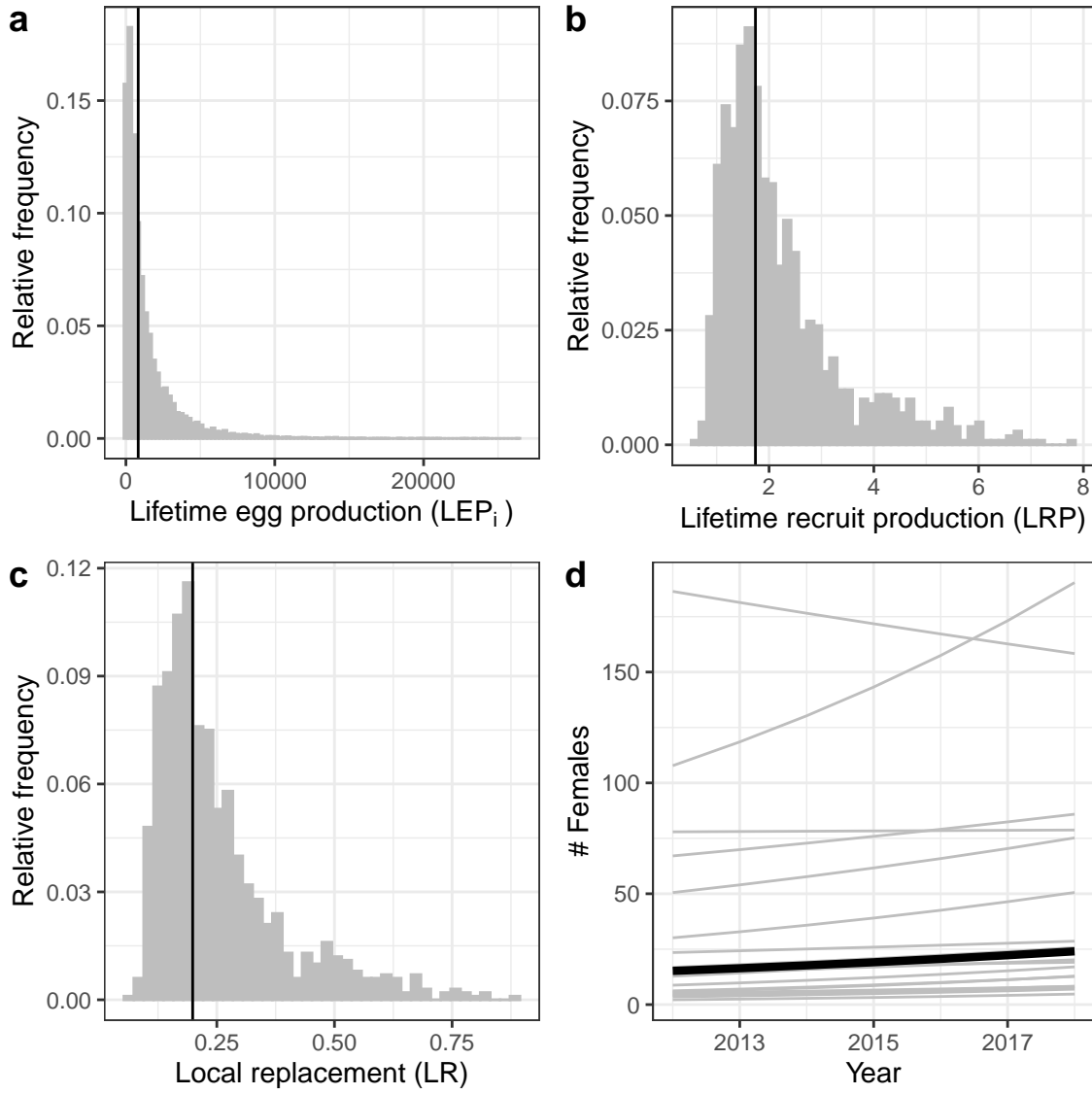


Figure 4: Estimates of a) individual-patch  $LEP_i$  (eqn. 7) for all patches with the point estimate averaged across patches ( $LEP_*$ , black line), b) average LRP across patches (eqn. 1), c) local replacement (LR, eqn. 4), showing the point estimate (black solid line) and range of estimates considering uncertainty in the inputs (grey). Estimates of LRP and LR include compensation for density-dependent mortality in early life stages. d) Estimated abundance of females over time at each individual patch (grey lines) and for an average patch (black line).

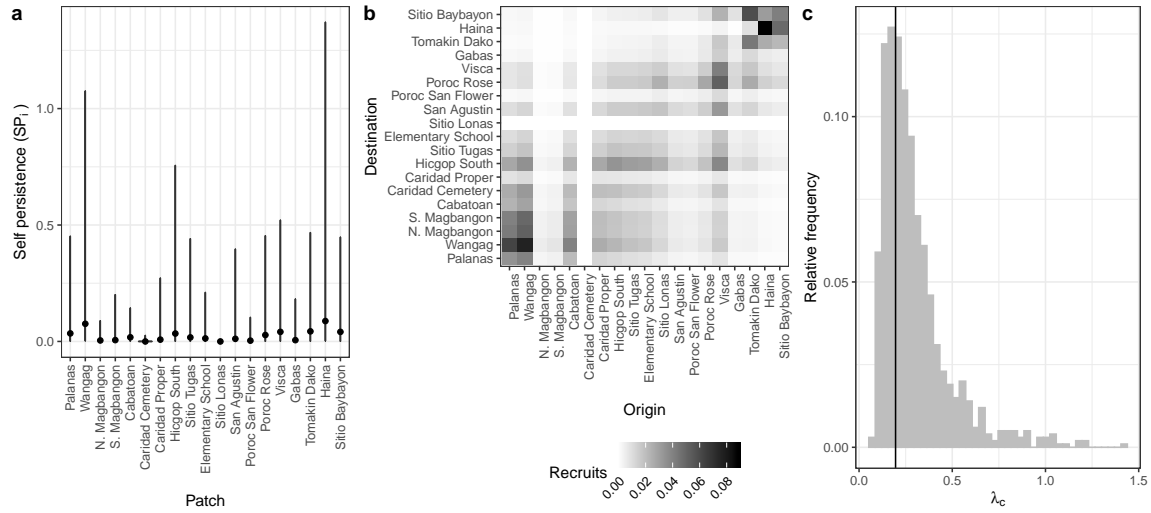


Figure 5: Values of a) self-persistence ( $SP_i$ , eqn. 2), b) realized connectivity among patches ( $C_{i,j}$ , eqn. 3), and c) network persistence ( $\lambda_c$ , first eigenvalue of eqn. 3). All estimates include compensation for density dependence in early life stages. For self-persistence (a) and network persistence (c), the best estimate is shown in black (point for (a), line for (c)) and the range of estimates considering uncertainty is shown in grey.

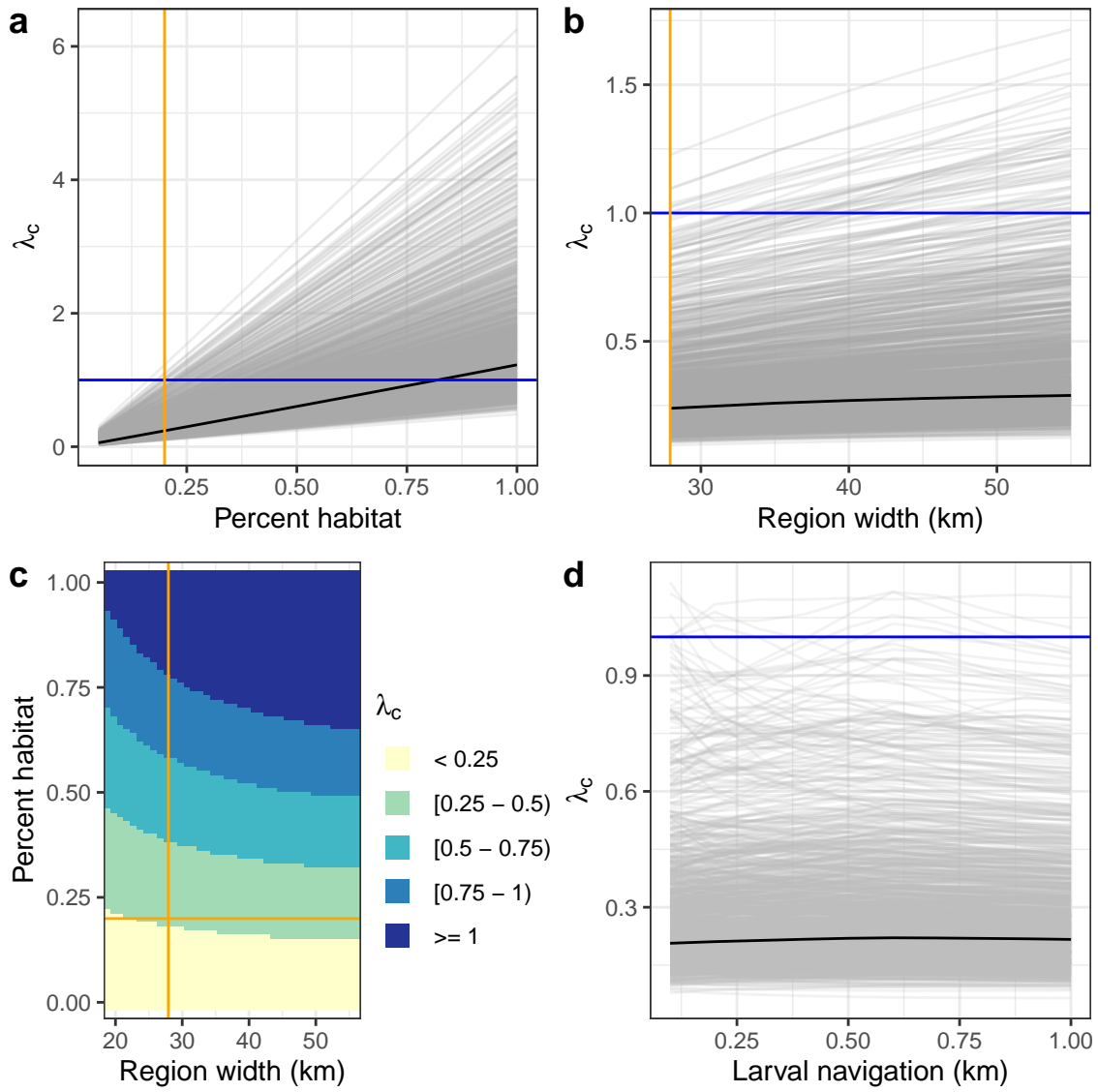


Figure 6: Sensitivity of network persistence ( $\lambda_c$ ) to a) the proportion of the sampling region that is habitat ( $P_s$ ), b) the width of a region with the same proportion habitat (20%), c) the region width and proportion habitat simultaneously, and d) larval navigation, where up to a 1 km buffer is added to the patch edges. The estimate is in black and each estimate with uncertainty is a grey line. The orange lines show the actual proportion habitat (20%) and region width (27 km) and the blue lines show the persistence threshold where  $\lambda_c = 1$ . Colors generated using Brewer (2020).

# Supporting Information

## 654 A Supplemental Methods

### A.1 Defining recruit and census stage

When assessing persistence, we must consider mortality and reproduction that occurs  
657 across the entire life cycle to determine whether an individual is replacing itself with  
an individual that reaches the same life stage (Burgess et al., 2014). We defined a  
recruit to be a juvenile individual that has settled on the reef within the previous  
660 year, which also encompasses the size of fish we were first able to sample (3.5–6.0 cm  
for parentage studies) (Fig. 1e, Appendix Fig. D.1). In theory, it does not matter  
how we defined recruit as long as we used the same definition in our calculations of  
663 both egg-recruit survival (eqn. 8) and LEP (eqn. 7). In our system, however, while  
it is straightforward to calculate LEP from any size, we did not have enough tagged  
recruits to reliably estimate survival from an egg to different recruit sizes. Instead, we  
666 chose the mean size of offspring matched in the parentage study as our best estimate  
of the size of a recruit ( $\text{size}_{\text{recruit}} = 4.4 \text{ cm}$ ) and tested sensitivity to different recruit  
sizes by sampling from a uniform distribution over the sizes the recruit stage covers  
669 (3.5–6.0 cm, Appendix Table C.1, Appendix Figs. D.11-D.14).

### A.2 Self persistence (SP)

Our equation for SP (eqn. 2) is a modification of that used in Burgess et al. (2014),  
672 which uses LEP to represent offspring produced and local retention (the number

of surviving recruits that disperse back to the natal patch divided by the number  
of eggs produced by the natal patch) to capture egg-recruit survival and dispersal  
675 combined: LEP x local retention  $\geq 1$ . We modify this to include egg-recruit survival  
in the offspring term instead, using LRP in place of LEP and probability of dispersal  
 $(p_{i,i})$  in place of local retention.

### 678 **A.3 Growth and survival**

To include size in the mark-recapture models for post-recruit survival ( $\phi$ ) and recapture  
probability ( $p_r$ ), we estimated sizes for fish in years when they were not recaptured.  
681 We used the growth model (eqn. 6) and the size recorded or estimated in the previous  
year to estimate the size of fish not recaptured in a particular year. Fish were not  
well-mixed at our patches, and divers needed to swim near an anemone to have a  
684 reasonable chance of capturing the fish on it. Therefore, we also included a distance  
effect on recapture probability (Appendix eqn. B.2, Appendix Table C.3). We used  
diver GPS tracks to estimate the minimum distance between a diver and the anemone  
687 where the fish was first caught for each tagged fish in each sample year.

We compared the fit of the models using a modified version of the Akaike information  
criterion that reduces the potential for overfitting with small sample sizes (AICc) and  
690 selected the model with the lowest AICc value (Appendix Table C.3).

### **A.4 Fecundity**

We used a size-dependent fecundity relationship determined using photos of egg  
693 clutches and females from field sampling, where the number of eggs per clutch ( $E_c$ ) is

exponentially related to the length in cm of the female ( $L$ ) with size effect  $\beta_l = 2.388$ ,  
intercept  $b = 1.174$ , and egg age effect  $\beta_e = -0.608$  dependent on if the eggs were old  
696 enough to have visible eyes. For fish larger or equal to the transition to female size  
 $L_f$ , we multiplied the number of eyed eggs per clutch by the number of clutches per  
year  $c_e = 11.9$  (estimate from Holtswarth et al., 2017) to get total annual fecundity  
699  $f$  for a female of length  $L$ :

$$f_L = \begin{cases} 0, & \text{if } L < L_f \\ c_e * e^{\beta_l \ln(L) + \beta_e [\text{eyed}] + b}, & L \geq L_f. \end{cases} \quad (\text{A.1})$$

We did not consider uncertainty in fecundity but did consider uncertainty in the  
transition size to breeding female (Appendix Methods A.9).

## 702 **A.5 Lifetime egg production (LEP)**

To compute LEP, we discretized time and size (in eqn. 7), using 100 time steps and  
100 equal size bins, and summed across the matrix. When entering the starting  
705 individual into the matrix, we used 0.1 as the standard deviation of size to spread  
out the starting individual across size bins. The size distribution at each time ( $v_{L,t}$ )  
represents the probability that the individual has survived and grown into each of  
708 the possible size categories. To account for differences in growth rates across fish,  
we used the size determined by the growth curve (eqn. 6) as the mean along with  
an estimate of spread ( $\text{size}_{sd}$ ) when projecting the size distribution of the fish in the  
711 next year. To estimate  $\text{size}_{sd}$ , we selected fish within 0.1 cm of the mean size at  
the first capture point for fish recaptured a year later (7.4–7.6 cm). We used the

standard deviation of the sizes of those fish when they were recaptured one year later  
714 as size<sub>sd</sub> (=1.45) (Appendix Table C.1).

LEP was estimated by patch ( $LEP_i$ ) because each patch has a different estimate  
of adult survival. We also present the average LEP across patches, noted as  $LEP_*$   
717 (Fig. 4b) and used to estimate average LRP and LR for the metapopulation (Fig.  
4c, d).

To estimate egg-recruit survival ( $S_e$ ), we used the expected lifetime egg production  
720 for a fish that has already survived to reach parent size (6.0 cm) so  $L_s$  in eqn. 7 =  
6.0, rather than 3.5. We used the average LEP for parent-sized fish across patches,  
noted as LEPP.

## 723 A.6 Accounting for density dependence

In 2015 and 2017, we did a more thorough survey of anemones at sampled patches  
and noted anemones occupied by yellowtail anemonefish, occupied by other species of  
726 anemonefish, and unoccupied by anemonefish. We found the proportion of anemones  
occupied by yellowtail anemonefish ( $p_A$ ) and the proportion of anemones unoccupied  
by any anemonefish ( $p_U$ ) for all patches combined and averaged across the two sample  
729 years. We used these average proportions to estimate the proportional increase (D)  
in unoccupied anemones if all anemones occupied by yellowtail anemonefish were  
unoccupied as described in the main text. We did not consider uncertainty in the  
732 effect of density dependence.

## A.7 Alternative geographies and larval navigation

### Larval navigation

735 In our sensitivity test for larval navigation and swimming abilities, we added a buffer ranging from 0–1 km to the edges of the destination patches when determining probability of dispersal between patches. To avoid overlapping shadows of effective  
738 area of neighboring patches, we added no more than half the distance between two adjacent patches to each patch. The buffers also changed the proportion of the sampling region that was habitat ( $P_h$ , see Appendix Methods A.8), as we considered  
741 the buffer areas to be habitat as well, and affected the scaling of recruits (Appendix Methods A.8) in egg-recruit survival (eqn. 8).

## A.8 Scaling up recruits

744 To estimate the total number of offspring produced by genotyped parents that survived to recruitment, we scaled up the number of matched offspring caught during sampling ( $R_m$ ) to account for recruits our sampling could have missed (Appendix  
747 Fig. D.2). We scaled up by 1) the cumulative proportion of habitat we sampled at our patches over time ( $P_h$ ) to account for recruits at anemones we did not sample,  
750 2) the probability of capturing a fish if we sampled its anemone ( $P_c$ ) to account for fish that escaped during sampling, 3) the proportion of the dispersal kernel from our patches covered within our sampling region ( $P_d$ ) to account for fish that dispersed outside of our sampling area (Appendix Fig. D.4), and 4) the proportion of our  
753 sampling region that was habitat ( $P_s$ ) to avoid counting mortality of fish dispersing to

non-habitat within our region twice. The latter term is important because mortality from dispersing to non-habitat is both in the estimate of total recruits (numerator of eqn. 8) and in the integrated dispersal kernel (eqn. 5).

### Proportion of habitat sampled ( $P_h$ )

We used tagged anemones to estimate the proportion of habitat we sampled within our patches (Appendix Table C.4). We tagged each anemone that was home to yellowtail anemonefish with a metal tag, which is relatively permanent and easy to re-sight (the anemone tag is visible above the anemone in Fig. 2c). We therefore considered the total number of metal-tagged anemones at a patch to be the habitat present. We used proportion of anemones rather than proportion of total patch area because anemones, and therefore habitat quality, were unevenly distributed across each patch; areas we did not visit typically had a lower anemone density than the areas we did sample.

To scale the number of sampled offspring from genotyped parents ( $R_m$ ) to account for areas of our patches we did not sample, we used the overall proportion habitat sampled across all patches and sampling years ( $P_h$ ). We summed the number of metal-tagged anemones we visited across all patches and years, then divided by the number of anemones we could have sampled (the sum of total metal-tagged anemones across all patches multiplied by the number of sampling years) (anemone numbers sampled by patch and year in Appendix Table C.4). We did not consider uncertainty in the proportion of habitat sampled.

### Probability of capturing a fish, from recapture dives ( $P_c$ )

We used the probability of capturing a fish to scale up the number of sampled  
787 offspring from genotyped parents ( $R_m$ ) to account for recruits we missed by failing  
to capture them. To estimate the probability of capturing a fish given that we  
sampled its anemone ( $P_c$ ), we used mark-recapture data from recapture dives done  
788 within a sampling season. During some of the sampling years, we intentionally  
re-sampled some locations within a few weeks of the original sampling dives. We  
assumed that the probability of recapturing a fish on a recapture dive was the same  
789 as capturing a fish on a sampling dive, essentially that there was no mortality in the  
weeks between dives and that the fish did not alter their behavior towards divers.  
For each recapture dive, we used GPS tracks of the divers to identify the anemones  
790 covered in the recapture dive and the set of PIT-tagged fish encountered on those  
anemones during the original sampling dives. We estimated the probability of capture  
791  $P_c$  as the number of tagged fish re-caught from the capture dive  $m_2$  divided by the  
total number of fish caught on the recapture dive  $n_2$ :  $P_c = \frac{m_2}{n_2}$ .

We used the mean  $P_c$  across all 14 recapture dives, covering 10 patches over three  
sampling seasons (2016, 2017, 2018), as our best estimate. Uncertainty details are  
792 in Appendix Methods A.9.

### Proportion of dispersal kernel area sampled ( $P_d$ )

To account for recruits that dispersed outside our sampling region, we found the  
795 proportion of the dispersal kernels from all parents that fell within our sampling

region (Appendix Fig. D.4). For each patch  $i$ , we found the area under the kernel ( $A_i$ ) from the center of the patch to the north edge of the sampling area ( $d_{N,i}$ )  
 798 (northern-most tagged anemone at Palanas, the northern-most patch) and from the center of the patch to the south edge of the sampling area ( $d_{S,i}$ ) (southern-most tagged anemone at Sitio Baybayon, the southern-most patch), then multiplied by  
 801 the number of genotyped parents at that patch ( $N_{g_i}$ ):

$$A_i = N_{g_i} \frac{e^{K_d \theta}}{2\Gamma(\frac{1}{\theta})} \left( \int_0^{d_N} e^{-(e^{K_d d})^\theta} dd + \int_0^{d_S} e^{-(e^{K_d d})^\theta} dd \right). \quad (\text{A.2})$$

We added the areas together, then divided by the total number of genotyped parents ( $N_g$ ) to get the proportion of the total dispersal kernel area covered by our  
 804 sampling region ( $P_d$ ):

$$P_d = \frac{\sum_{i=1}^{19} A_i}{N_g}. \quad (\text{A.3})$$

We did not consider uncertainty in  $P_d$ .

### Proportion habitat in sampling area ( $P_s$ )

807 To avoid implicitly counting mortality due to larvae settling on non-habitat twice — once in scaling up our matched recruits (who settled on habitat) and once in integrating the dispersal kernel — we scaled the estimate of total recruits produced  
 810 by parents on our patches by the proportion of our sampling region that was habitat ( $P_s$ ). We found  $P_s$  by summing the lengths of all the patches, which run approximately north-south, and dividing by the total north-south distance of our sampling region,

813 giving  $P_s = 0.20$ . We assumed that larvae were unable to navigate to habitat if they  
dispersed to an unsuitable area but relaxed that assumption in our sensitivity tests  
(Appendix Methods A.7) because anemonefish larvae do likely have some ability  
816 both to sense good settlement areas by detecting host anemones (Elliott et al., 1995;  
Arvedlund et al., 1999) or conspecifics (e.g., Lecchini et al., 2005, for coral reef fish  
more broadly), and to swim in a particular direction (e.g., Bellwood and Fisher,  
819 2001; Fisher, 2005).

## A.9 Characterizing uncertainty

### Dispersal kernel

822 To account for uncertainty in the dispersal kernel, we used sets of the shape parameter  
 $\theta$  and the scale parameter  $K_d$  that represented the span of the 95% confidence interval  
when  $K_d$  and  $\theta$  were estimated jointly (Appendix Table C.1, Fig. 3a, Catalano et al.,  
825 in press). We randomly sampled pairs of  $\theta$  and  $K_d$  parameters from within the 95%  
confidence intervals, weighted by the log-likelihood.

### Growth

828 We used the first and second capture lengths for fish that were recaptured after a year  
(within 345 to 385 days) to estimate  $L_\infty$  and  $k$  (using eqn. 6). For fish recaptured  
more than once, we randomly selected only one recapture period from each to use  
831 to estimate the von Bertalanffy parameters and repeated the random selection and  
estimate 1000 times. We found the mean estimates ( $L_\infty = 10.70$  cm,  $k = 0.864$ ) and  
mean standard error of those fits, then sampled uniformly from within the average

<sup>834</sup> 95% range to generate a set of von Bertalanffy growth curves to use in our LEP calculations (Fig. 3b, Appendix Fig. D.3b, Appendix Table C.1).

### **Survival ( $\phi$ )**

<sup>837</sup> We incorporated uncertainty in adult survival by sampling uniformly from within the 95% confidence limits for the patch-based survival estimates and size effect on survival as estimated by the lowest AICc model from MARK (Appendix Table C.2,  
<sup>840</sup> Appendix Fig. D.5). For the simulations for the alternative geographies and larval navigation, we used the survival estimate and 95% range for the patch with median survival (the Elementary School patch) (Appendix Table C.1).

### **<sup>843</sup> Size of transition to female ( $L_f$ )**

To incorporate uncertainty in the size at which male fish transition to female ( $L_f$ ), we sampled with replacement directly from the sizes at which recaptured fish were first captured as female (5.2–12.7 cm) (Fig. 3d). Reproductive output is only counted once fish reach the female stage, so  $L_f$  affects fecundity (Appendix eqn. A.1) and therefore the fecundity kernel in calculating lifetime egg production ( $f_L$  in eqn. 7).

### **<sup>849</sup> Recruit size (size<sub>recruit</sub>)**

We incorporated uncertainty in the size of a recruit (size<sub>recruit</sub>) by sampling from a uniform distribution across the ranges of possible sizes of recruits for the parentage analysis (3.5–6.0 cm) (Appendix Fig. D.3a). Recruit size enters into LEP as the starting size of the individual fish in eqn. 7.

## Probability of capturing a fish ( $P_c$ )

855 To consider uncertainty in the probability of capturing a fish given that we sampled  
its anemone ( $P_c$ ), we represented the probability of capture as a beta distribution,  
using the mean  $\mu_{P_c}$  and variance  $V_{P_c}$  of the set of 14 values calculated from individual  
858 recapture dives to find the appropriate  $\alpha_{P_c}$  and  $\beta_{P_c}$  parameters, where

$$\alpha_{P_c} = \left( \frac{1 - \mu_{P_c}}{V_{P_c}} - \frac{1}{\mu_{P_c}} \right) \mu_{P_c}^2 \quad (\text{A.4})$$

$$\beta_{P_c} = \alpha_{\mu_{P_c}} \times \frac{1}{\mu_{P_c} - 1}. \quad (\text{A.5})$$

The mean of the individual capture probability values was  $\mu_{P_c} = 0.56$ , with variance  $V_{P_c} = 0.069$ , giving beta distribution parameters  $\alpha_{P_c} = 1.44$  and  $\beta_{P_c} = 1.13$ .

861 We sampled 1000 values from the beta distribution, then truncated the sample to include only values larger or equal to the lowest value of  $P_c$  estimated from an individual dive (0.20), to avoid unrealistically low values randomly sampled from the 864 distribution. We then sampled with replacement from the truncated set to get a vector of 1000 values (Appendix Fig. D.3c).  $P_c$  is one of the scaling factors in the estimate of egg-recruit survival (eqn. 8), accounting for recruits we missed by failing 867 to capture them.

## Lifetime Egg Production (LEP)

Uncertainty in lifetime egg production enters through adult survival, growth, and  
870 the size of a recruit (Appendix Methods A.9), all of which affect the size distribution  
across time  $v_{L,t}$  in eqn. 7. Additionally, uncertainty in the size of transition to female  
( $L_f$ , Appendix Methods A.9) affects the fecundity kernel  $f_L$  in eqn. 7. We show the  
873 contribution of uncertainty of each input in Appendix Fig. D.11.

## Egg-recruit survival ( $S_e$ )

In estimating egg-recruit survival ( $S_e$ ), we considered uncertainty in the number of  
876 offspring assigned to parents ( $R_m$ ) and in the probability of capturing a fish ( $P_c$ ). For  
offspring assigned to parents, we generated a set of values for the number of assigned  
offspring using a random binomial, with the number of genotyped offspring (791) as  
879 the number of trials and the assignment rate from the parentage analysis (0.090) as  
the probability of success on each trial (Catalano et al., in press) (Appendix Fig.  
D.3d). Uncertainty in probability of capture  $P_c$  is described in Appendix Methods  
882 A.9. We show the contribution of uncertainty of each input in Appendix Fig. D.13.

## B Supplemental Results

### B.1 Parentage

885 From the genetic work and parentage analysis done in Catalano et al. (in press), we  
genotyped 1729 potential parents, genotyped 791 potential offspring (recruits), and  
matched 71 offspring to parents, with an assignment rate of 9%. In estimates with  
888 uncertainty, the middle 95% of the distribution of matched offspring was 55 to 87  
(Appendix Fig. D.3d, Appendix Table C.1).

The combined number of potential parents and potential offspring is higher than  
891 the number of genotyped fish because some fish are included as both a potential  
offspring and a potential parent (in different years).

### B.2 Dispersal kernel

894 We used the dispersal kernel estimated for all years together in Catalano et al. (in  
press) (eqn. 5), with  $K_d = -2.51$  and  $\theta = 1.49$ . Using the 95% confidence surface  
when  $K_d$  and  $\theta$  were estimated jointly to incorporate uncertainty (Appendix Methods  
897 A.9),  $K_d$  ranged from  $-2.86$  to  $-1.82$  and  $\theta$  from  $0.87$  to  $2.46$  (Fig. 3a, Appendix  
Table C.1).

### B.3 Growth

900 From the mark-recapture analysis of tagged and genotyped fish, we estimated mean  
values of  $L_\infty = 10.70$  cm with uncertainty bounds of 9.0–12.8 cm using the 95%  
confidence bounds with average standard error across fits and  $k = 0.864$  with

903 uncertainty bounds 0.73–1.01 for the von Bertalanffy growth curve parameters (eqn.  
6, Fig. 3b, Appendix Table C.1).

## B.4 Survival

906 The best model for post-recruitment annual survival  $\phi$  on a log-odds scale had a positive size effect ( $b_a = 0.15 \pm 0.029$  SE) with intercepts  $b_{\phi_i}$  varying by patch (Appendix eqn. B.1, Appendix Fig. D.5, Appendix Table C.2):

$$\ln\left(\frac{\phi}{1-\phi}\right) = b_{\phi_i} + b_a \text{size}. \quad (\text{B.1})$$

909 The accompanying best model for recapture probability  $p_r$  on a log-odds scale had a negative effect of size ( $b_1 = -0.16 \pm 0.09$  SE) and a negative effect of diver distance  $d$  from the capture anemone ( $b_2 = -0.15 \pm 0.02$  SE), with intercept  $b_{p_r} = 2.14 \pm 0.87$   
912 SE (Appendix eqn. B.2, Appendix Fig. D.6):

$$\ln\left(\frac{p_r}{1-p_r}\right) = b_{p_r} + b_1 \text{size} + b_2 d. \quad (\text{B.2})$$

This suggests divers were less likely to recapture larger fish, who are stronger swimmers and more likely to flee when divers approach, and those at anemones far  
915 from areas sampled.

## B.5 Scaling factors

The proportion of habitat at patches sampled over time ( $P_h$ ) was 0.41, the proportion  
918 of the region that was habitat ( $P_s$ ) was 0.20, the proportion of the dispersal kernel

that was within the sampling region ( $P_d$ ) was 0.57, and the probability of capturing a fish given that its anemone was sampled ( $P_c$ ) was 0.56, with middle 95% 0.22–0.97  
921 (Appendix Fig. D.3c, Appendix Table C.1).

## B.6 Lifetime egg production (LEP)

We calculated an average value of LEP across patches (LEP<sub>\*</sub>) of 827 [266, 3213] eggs  
924 (Fig. 4a), with best estimate values at individual patches that ranged from 0 to 1760 eggs (Appendix Table C.5). Uncertainty in adult survival had the largest effect on LEP (Appendix Fig. D.11), which corresponds to longer-surviving individuals having  
927 more opportunities to reproduce at larger sizes.

## B.7 Egg-recruit survival ( $S_e$ )

We estimated egg-recruit survival  $S_e$  to be 0.002 [ $5 \times 10^{-4}$ , 0.01] when we accounted  
930 for density dependence in our data. Uncertainty in the size of transition to breeding female  $L_f$  had the largest effect on egg-recruit survival (Appendix Fig. D.13); the larger the transition size to female, the fewer tagged eggs we estimated were produced  
933 by our genotyped parents and the higher the estimate of egg-recruit survival. This differs from our finding above that adult survival had the largest effect on LEP because the starting size of the individual considered is lower when we estimate LEP  
936 for a recruit (4.4 cm, 3.5–6.0 cm range) than for a parent (6.0 cm). Fish considered parents in our parentage analysis have already survived one or more years since recruiting so the transition to breeding female plays a larger role in the number of  
939 eggs they are likely to produce than for fish who have just recruited.

## B.8 Persistence metrics without compensation for density dependence

942 Estimating persistence metrics without compensating for density dependence in our  
943 data (presented with a subscript D) gave us an understanding of whether individuals  
944 at our patches were able to replace themselves and whether our patches would persist  
945 in isolation at the current abundance levels, rather than at low abundance. Without  
946 compensation for early life density dependence, all of our metrics showed that the  
947 set of patches we sampled was less likely to persist as an isolated network than the  
948 metrics for low abundance. We estimated egg-recruit survival ( $S_{eD}$ ) to be 0.001  
949 [ $3 \times 10^{-4}$ , 0.005] and average lifetime recruit production across patches ( $LRP_D$ ) to  
950 be 0.96 [0.51, 3.07], with 52% of  $LRP_D$  estimates  $\geq 1$  (Appendix Fig. D.9a). Our  
951 estimate of local replacement ( $LR_D$ ), which estimates replacement for recruits from  
952 our patches returning to our patches implicitly including dispersal, was 0.11 [0.06,  
953 0.35] (Appendix Fig. D.9b).

954 When we calculated LR using all arriving recruits to our patches, however, rather  
955 than just those originating there, the best estimate was  $> 1$  (1.22), suggesting that  
956 there was recruit-recruit replacement at our patches when we included immigrant  
957 recruits, even at current population levels when density dependence was present.

958 We did not find any patches with a best estimate of  $SP_D \geq 1$  or with uncertainty  
959 bounds that reached or exceeded 1 (Appendix Figs. D.10a). Our best estimate of  
960 the dominant eigenvalue of the realized connectivity matrix  $\lambda_{cD}$  was 0.11 [0.06, 0.47]  
961 with 0% of estimates where  $\lambda_{cD} \geq 1$  (Appendix Fig. D.10c).

## C Supplemental Tables

Table C.1: Summary of parameter symbols, definitions, and values, including sections and equations where each is described in detail.

Parameter	Description	Best estimate (uncertainty bounds)	Uncertainty origin	Details	Notes
<i>Dispersal and demographics</i>					
$K_d$	scale parameter in dispersal kernel	-2.51 (-2.86, -1.82)	drawn from joint 95% confidence limits with $\theta$ , weighted by log-likelihood	eqn. 5, Appendix Methods A.9, Appendix Results B.2	estimated Catalano et al. (in press)
$\theta$	shape parameter in dispersal kernel	1.49 (0.87, 2.46)	drawn from joint 95% confidence limits with $K_d$ , weighted by log-likelihood	eqn. 5, Appendix Methods A.9, Appendix Results B.2	estimated Catalano et al. (in press)
$L_\infty$	average asymptotic size (cm) in von Bertalanffy growth curve	10.7 cm (9.0, 12.8)	average 95% confidence limits of growth curves estimated with different pairs of fish	eqn. 6, Appendix Methods A.3, A.9, Appendix Results B.3	
$k$	growth coefficient in von Bertalanffy growth curve	0.864 (0.732, 1.01)	average 95% confidence limits of growth curves estimated with different pairs of fish	eqn. 6, Appendix Methods A.3, A.9, Appendix Results B.3	

size <sub>recruit</sub>	size of a recruit	4.4 cm (3.5–6.0)	sampled from a uniform distribution to match the range of offspring sizes for parentage analyses	Appendix Methods A.1, A.9	used as starting size of fish in calculation of LEP (eqn. 7)
$b$	intercept at 0 cm for size-fecundity relationship	1.174 eggs	no uncertainty	Appendix eqn. A.1, Appendix Methods A.4	
$\beta_l$	size effect for size-fecundity relationship	2.388 $\frac{\text{eggs}}{\text{cm}}$	no uncertainty	Appendix eqn. A.1, Appendix Methods A.4	
$\beta_e$	egg age effect in fecundity	-0.608	no uncertainty	Appendix eqn. A.1, Appendix Methods A.4	egg age was determined by the presence of visible eyes (eyed vs. non-eyed)
$c_e$	number of egg clutches per year	11.9	no uncertainty	Appendix eqn. A.1, Appendix Methods A.4	Holtswarth et al. (2017)

$\text{size}_{\text{sd}}$	spread in sizes of fish one year later	1.45	no uncertainty	used in estimating LEP, Appendix Methods A.5	estimated from recapture data
parent size	size of fish used to estimate LEP for parents (LEP <sub>p</sub> )	6.0 cm	no uncertainty	Appendix Methods A.5	used in estimating egg-recruit survival ( $S_e$ , eqn. 8)
$R_m$	number of offspring matched to genotyped parents	71 [55, 87]	middle 95% of distribution from random binomial for each genotyped offspring using the assignment rate from the parentage analysis (9%)	Appendix Methods A.9	used in calculating egg-recruit survival ( $S_e$ , eqn. 8)
genotyped offspring	number of recruits genotyped	791	no uncertainty	Appendix Results B.1	used to find mean recruit size ( $\text{size}_{\text{recruit}}$ ), estimate metrics with immigrants included

$N_g$	potential parents genotyped	1729	no uncertainty	Appendix Results B.1	used to find proportion of dispersal kernel area sampled ( $P_d$ , Appendix Methods A.8), egg-recruit survival ( $S_e$ , eqn. 8)
$L_f$	size of transition to female	9.3 cm (5.2, 12.7)	sampled with replacement from transition sizes for recaptured fish	Appendix eqn. A.1, Appendix Methods A.9	used to find fecundity (Appendix eqn. A.1)
$b_{\phi,i=ES}$	intercept at size = 0 cm for survival at Elementary School patch	-1.88 (-3.33, -0.44)	sampled from within 95% confidence limits from MARK estimates	Appendix eqn. B.1, Appendix Methods A.3, A.9, Appendix Results B.4	patch with median survival, used in proportion habitat, region width, and larval navigation sensitivity tests
$b_a$	size effect for survival	0.15 (0.10, 0.21)	sampled from within 95% confidence limits from MARK estimates	Appendix eqn. B.1, Appendix Methods A.3, A.9, Appendix Results B.4	

*Scaling factors*

D	proportional increase in unoccupied anemones to account for density-dependence at settlement	1.18	no uncertainty	section “Accounting for density-dependence”, Appendix Methods A.6	used to scale recruits for egg-recruit survival ( $S_e$ , eqn. 8)
$p_A$	proportion anemones occupied by yellowtail anemonefish	0.37	no uncertainty	Appendix Methods A.6	
$p_U$	proportion anemones unoccupied by anemonefish	0.46	no uncertainty	Appendix Methods A.6	
$P_h$	cumulative proportion of habitat in patches sampled	0.41	no uncertainty	Appendix Methods A.8	used to scale recruits for egg-recruit survival ( $S_e$ , eqn. 8)
$P_s$	proportion of region that was habitat	0.20	no uncertainty	Appendix Methods A.8	used to scale recruits for egg-recruit survival ( $S_e$ , eqn. 8)
$P_d$	proportion dispersal kernel area in sampling region	0.57	no uncertainty	Appendix Methods A.8	used to scale recruits for egg-recruit survival ( $S_e$ , eqn. 8)
$P_c$	probability of capturing a fish	0.56	sampled from a beta distribution	Appendix Methods A.8, A.9	used to scale recruits for egg-recruit survival ( $S_e$ , eqn. 8)



Table C.2: Table with patch-specific survival values ( $\phi_i$ ) on a log-odds scale (used in Appendix eqn. B.1), where the intercept is for post-recruit survival for a fish of size 0 cm. The intercept for each patch is the intercept for Cabatoan plus the additional intercept value for that patch, shown in the table.

Patch	Intercept	Standard error	Confidence limits	Notes
Cabatoan	-1.78	0.33	-2.42 to -1.14	
Caridad Cemetery	-19.66	0.00	-19.66 to -19.66	addition to Cabatoan intercept
Elementary School	-0.11	0.41	-0.92 to 0.69	addition to Cabatoan intercept
Gabas	-0.42	0.58	-1.55 to 0.72	addition to Cabatoan intercept
Haina	0.12	0.35	-0.57 to 0.81	addition to Cabatoan intercept
Higcop South	-0.06	0.46	-0.96 to 0.84	addition to Cabatoan intercept
N. Magbangon	-1.31	0.38	-2.05 to -0.57	addition to Cabatoan intercept
Palanas	0.24	0.26	-0.26 to 0.75	addition to Cabatoan intercept
Poroc Rose	-0.19	0.44	-1.05 to 0.68	addition to Cabatoan intercept
Poroc San Flower	-0.52	0.48	-1.45 to 0.42	addition to Cabatoan intercept
San Agustin	-0.47	0.50	-1.45 to 0.42	addition to Cabatoan intercept
Sitio Baybayon	0.02	0.26	-0.49 to 0.52	addition to Cabatoan intercept
S. Magbangon	-1.08	0.48	-2.02 to -0.14	addition to Cabatoan intercept
Tomakin Dako	0.39	0.33	-0.25 to 1.03	addition to Cabatoan intercept
Visca	0.33	0.35	-0.36 to 1.01	addition to Cabatoan intercept
Wangag	0.35	0.25	-0.15 to 0.85	addition to Cabatoan intercept

Table C.3: Table showing the set of models considered in MARK for survival ( $\phi$ , from Appendix eqn. B.1) and recapture probability ( $p_r$ , from Appendix eqn. B.2), including effects of fish size ( $L$ ), minimum distance from diver to the anemone where the fish was first caught during surveys ( $D_m$ ), year ( $t$ ), and patch ( $i$ ), and their relative AICc scores.

<b>Model</b>	<b>Model description</b>	<b>AICc</b>	<b>dAICc</b>
$\phi \sim L + i, p_r \sim L + D_m$	survival: size + patch, recapture: size + distance	3104.1	0
$\phi \sim i, p_r \sim L + D_m$	survival: patch, recapture: size + distance	3127.2	23.1
$\phi \sim i, p_r \sim D_m$	survival: patch, recapture: distance	3127.2	23.1
$\phi \sim L, p_r \sim L + D_m$	survival: size, recapture: size + distance	3139.9	35.8
$\phi \sim L, p_r \sim D_m$	survival: size, recapture: distance	3141.6	37.5
$\phi, p_r \sim L + D_m$	survival: constant, recapture: size + distance	3168.4	64.3
$\phi, p_r \sim D_m$	survival: constant, recapture: distance	3169.3	65.2
$\phi \sim t, p_r$	survival: time, recapture: constant	3243.9	139.8
$\phi \sim i, p_r$	survival: patch, recapture: constant	3254.4	150.3
$\phi, p_r \sim t$	survival: constant, recapture: time	3274.0	169.9
$\phi \sim L, p_r \sim L$	survival: size, recapture: size	3345.1	241.0
$\phi, p_r$	survival: constant, recapture: constant	3382.7	278.6

Table C.4: Table showing the percent of anemones surveyed at each patch, ordered from north to south, in each sampling year.

		% Habitat surveyed						
Patch	# Total anems	2012	2013	2014	2015	2016	2017	2018
Palanas	138	29	57	48	61	85	86	86
Wangag	291	18	33	42	35	27	49	69
N. Magbangon	105	5	12	40	63	64	0	5
S. Magbangon	34	41	56	32	0	65	0	71
Cabatoan	26	42	58	58	65	73	0	62
Caridad Cemetery	4	0	75	50	0	50	50	50
Caridad Proper	4	0	100	0	0	0	0	0
Hicgop South	18	0	67	28	28	56	83	78
Sitio Tugas	8	0	100	0	0	0	0	0
Elementary School	7	0	100	43	100	100	86	100
Sitio Lonas	1	100	100	0	0	0	0	0
San Agustin	18	89	61	72	61	100	89	72
Poroc San Flower	11	100	82	73	73	55	82	64
Poroc Rose	13	100	100	69	31	23	69	69
Visca	13	100	100	23	38	62	85	62
Gabas	9	0	0	0	44	44	67	0
Tomakin Dako	48	0	25	23	38	35	60	69
Haina	104	0	6	13	13	10	56	80
Sitio Baybayon	259	0	14	30	34	30	41	81
Overall	1111	16	32	36	39	42	48	67

Table C.5: Table showing patch-specific estimates of lifetime egg production ( $LEP_i$ ), lifetime recruit production ( $LRP_i$ ), and self persistence ( $SP_i$ )

Patch	$LEP_i$	$LRP_i$	$SP_i$
Palanas	1383	2.91	0.03
Wangag	1642	3.45	0.08
N. Magbangon	133	0.28	0.004
S. Magbangon	183	0.39	0.006
Cabatoan	933	1.96	0.02
Caridad Cemetery	0	0	0
Caridad Proper	781	1.64	0.008
Hicop South	848	1.78	0.03
Sitio Tugas	781	1.64	0.02
Elementary School	781	1.64	0.01
Sitio Lonas	781	1.64	0
San Agustin	445	0.92	0.01
Poroc San Flower	415	0.87	0.004
Poroc Rose	694	1.46	0.03
Visca	1586	3.34	0.04
Gabas	483	1.02	0.006
Tomakin Dako	1760	3.70	0.04
Haina	1130	2.38	0.09
Sitio Baybayon	959	2.02	0.04

963 D Supplemental Figures

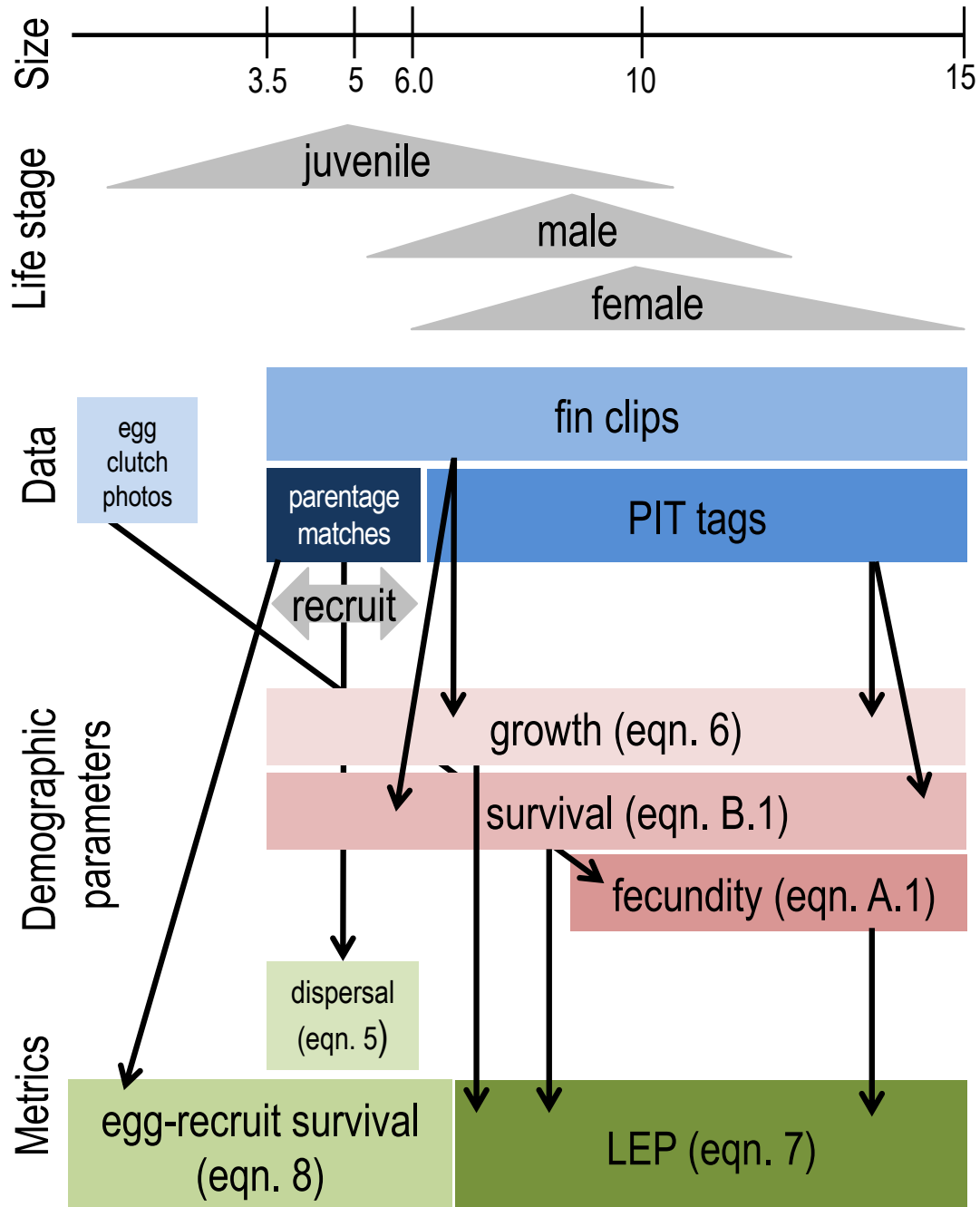


Figure D.1: The data collected for fish <sup>69</sup> at each life stage and how they match to the equations and metrics estimated. We considered recruits to be offspring in their first year of settlement, represented by the 3.5–6.0 cm size range (Appendix Methods A.1).

## How could we have missed potential recruits originating from our patches?

- 1) Failed to catch recruit when sampling ( $P_c$ )
- 2) Missed sampling some habitat areas within our patches ( $P_h$ )
- 3) Recruit dispersed outside our study region ( $P_d$ )
- 4) Recruit dispersed to non-habitat within our region ( $P_s$ )
- 5) Recruit died due to density-dependent competition with other settlers (D)

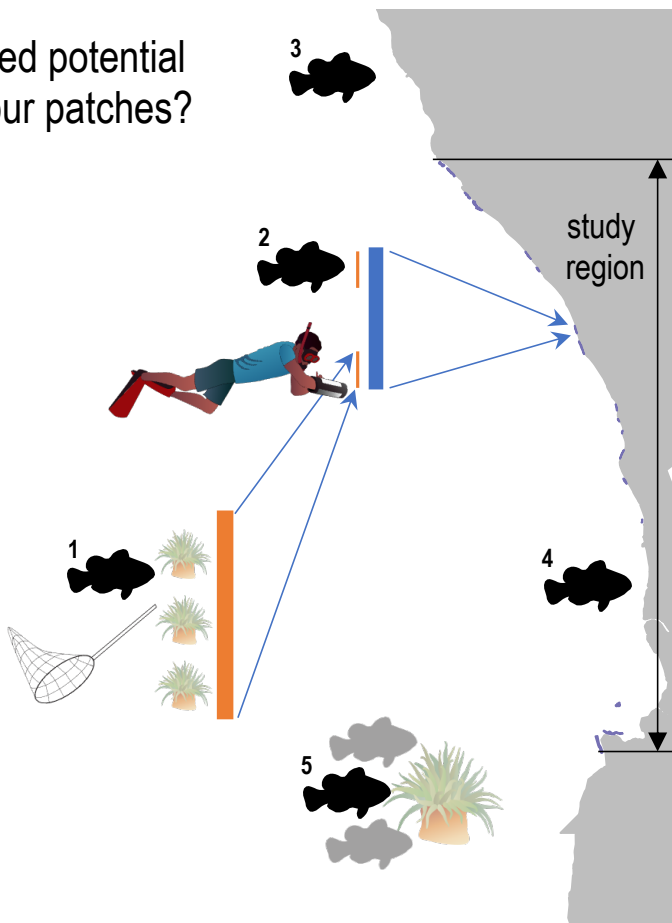


Figure D.2: Schematic of five ways we could have missed recruits while sampling. We used these factors to scale up our raw estimate of recruits from matched offspring (Appendix Methods A.8). Diver image created by Tracey Saxby, Integration and Application Network, University of Maryland Center for Environmental Science ([ian.umces.edu/imagelibrary/](http://ian.umces.edu/imagelibrary/)).

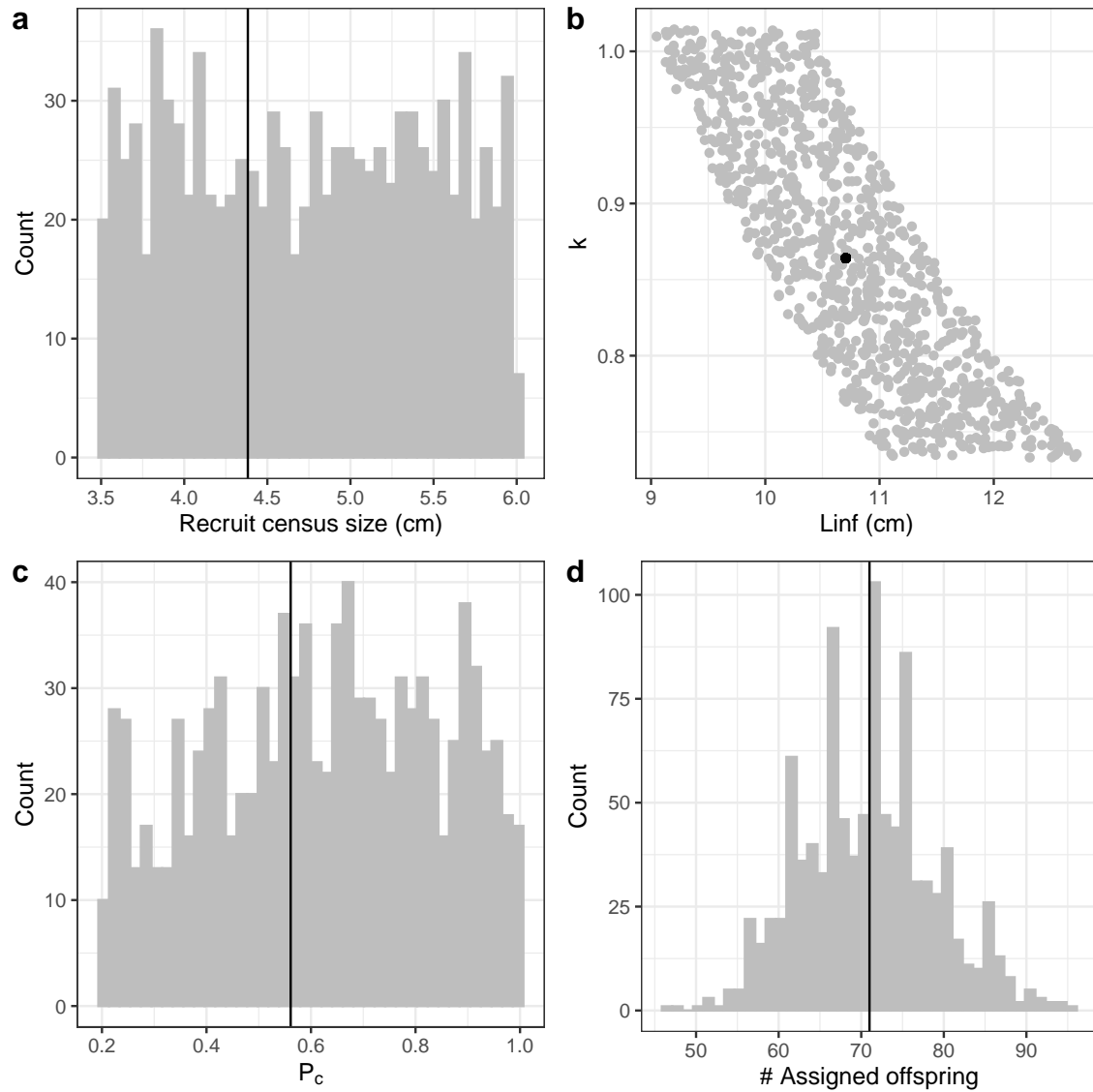


Figure D.3: Range of parameter inputs for uncertainty runs with all uncertainty included, where the black line or point is the value used for the best estimate: a)  $\text{size}_{\text{recruit}}$ , the census size for recruits after egg-recruit survival; b) the parameters  $L_{\infty}$  and  $k$  of the von Bertalanffy growth model; c)  $P_c$ , the probability of capturing a fish; d)  $R_m$ , the number of offspring assigned back to parents in the parentage analysis.

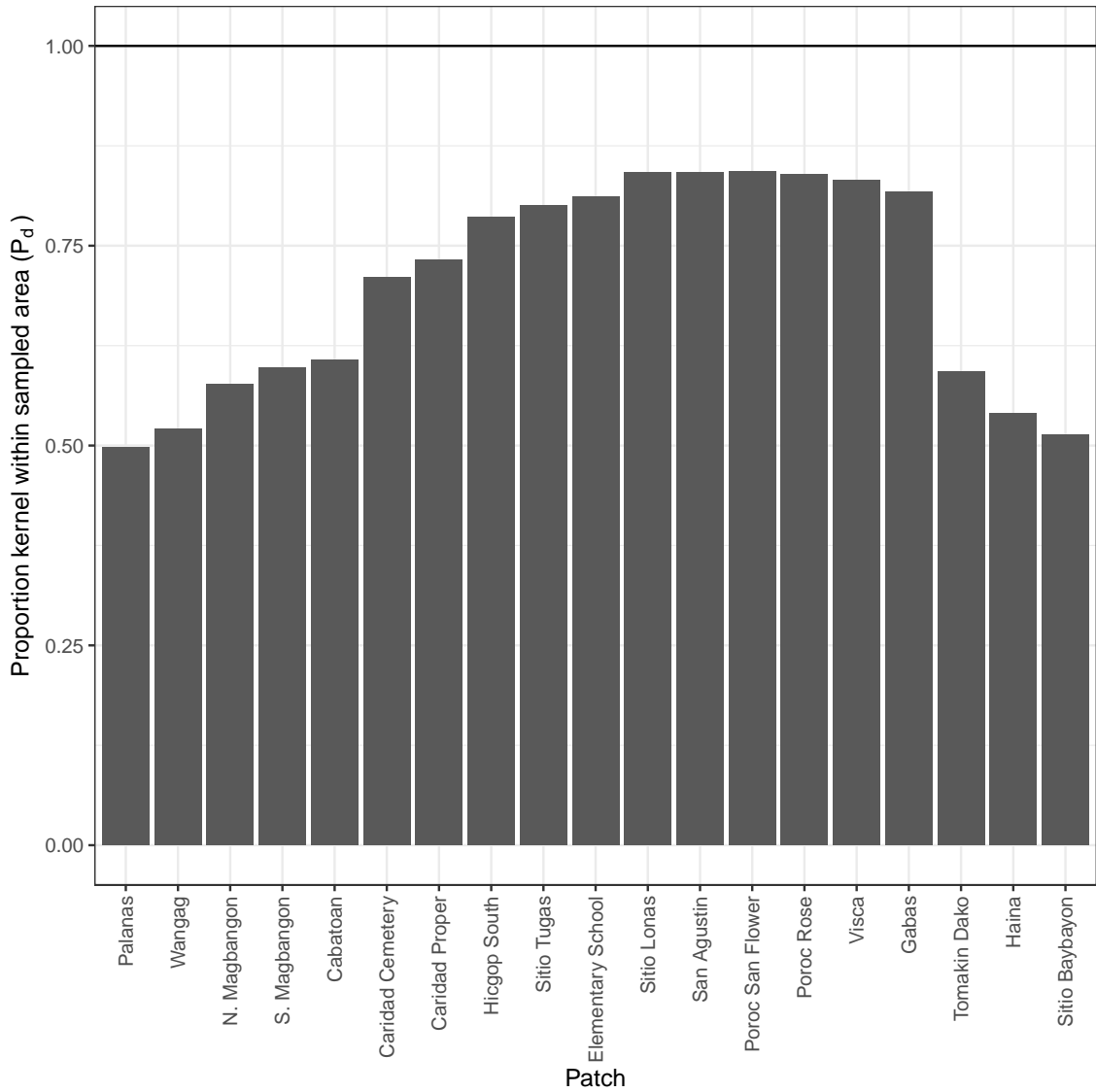


Figure D.4: Proportion of the dispersal kernel area from the center of each patch covered by our sampling region ( $\frac{A_i}{N_{g,i}}$  from Appendix eqn. A.3). The overall proportion ( $P_d$ ) is weighted by the number of parents at each patch.

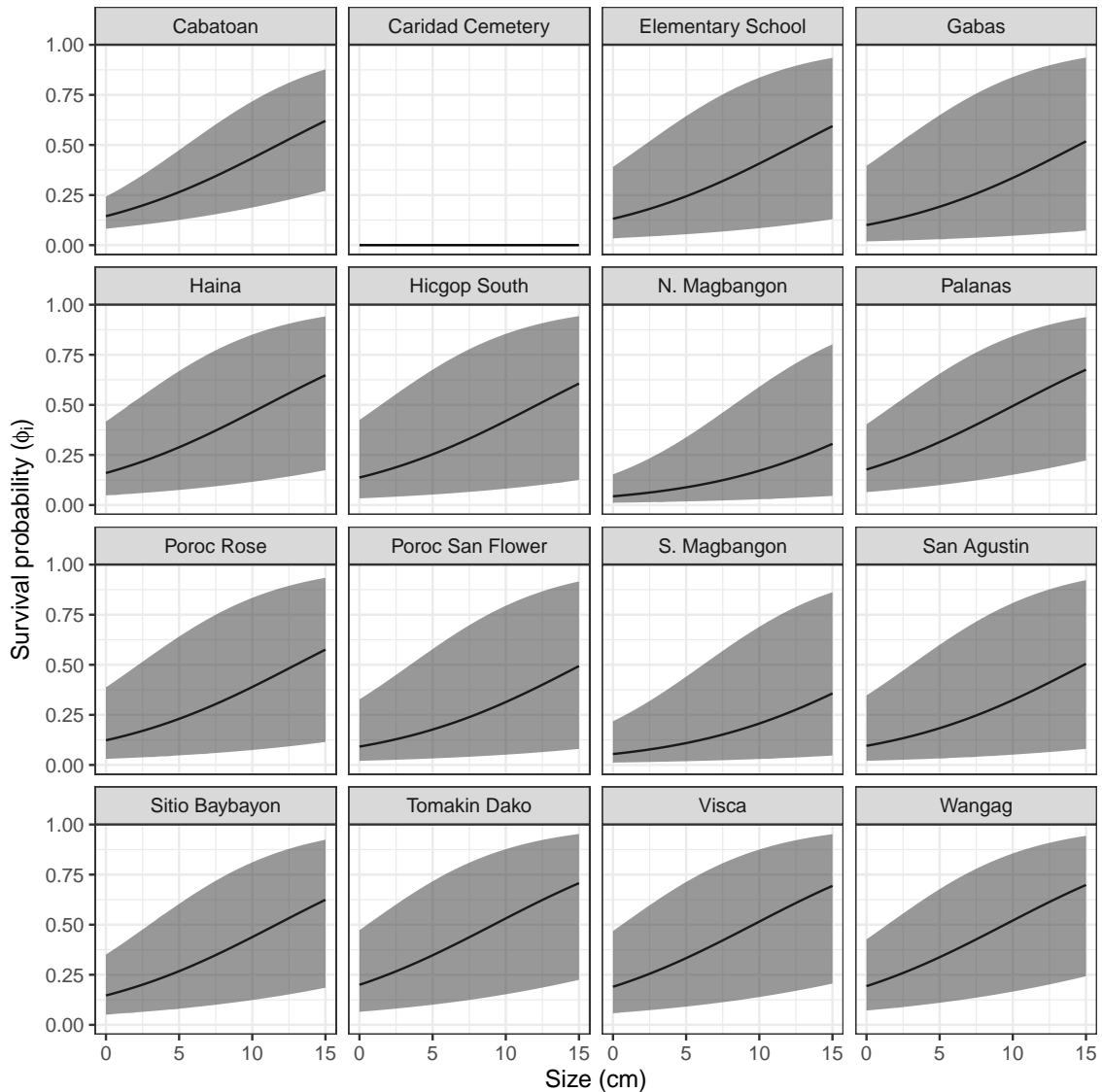


Figure D.5: Annual post-recruit survival ( $\phi$ ) by fish size at each patch, detailed in Appendix Methods A.3, A.9, and Appendix Results B.4.

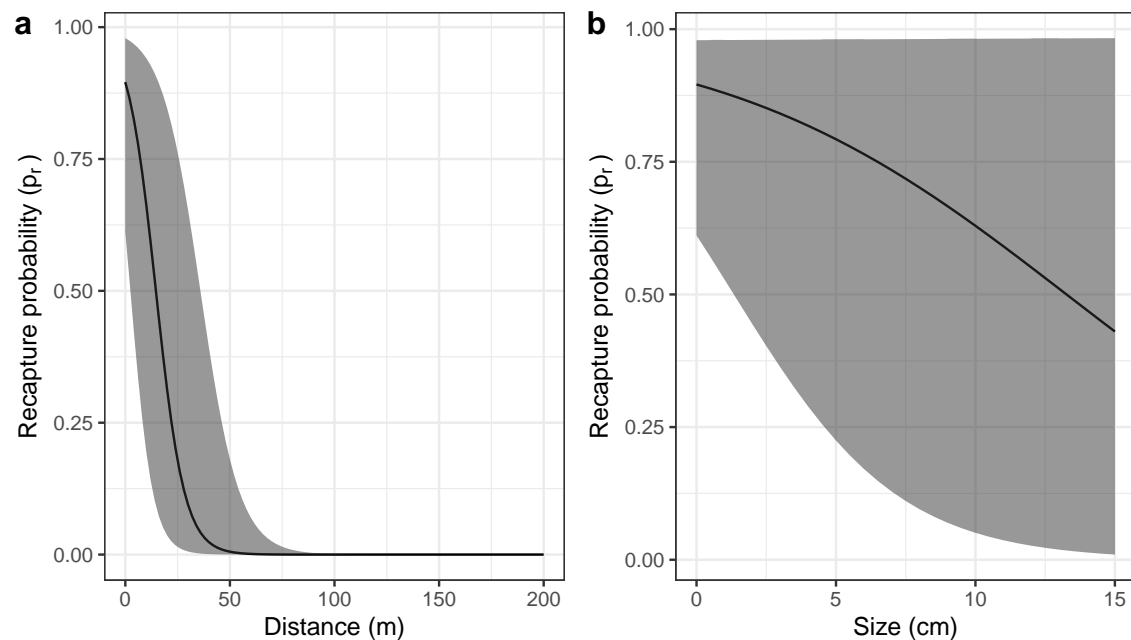


Figure D.6: Effects of a) minimum distance between divers and the anemone where the fish was first caught and b) fish size on recapture probability  $p_r$ , estimated along with survival in a mark-recapture analysis (Appendix Methods A.3 and Appendix Results B.4).

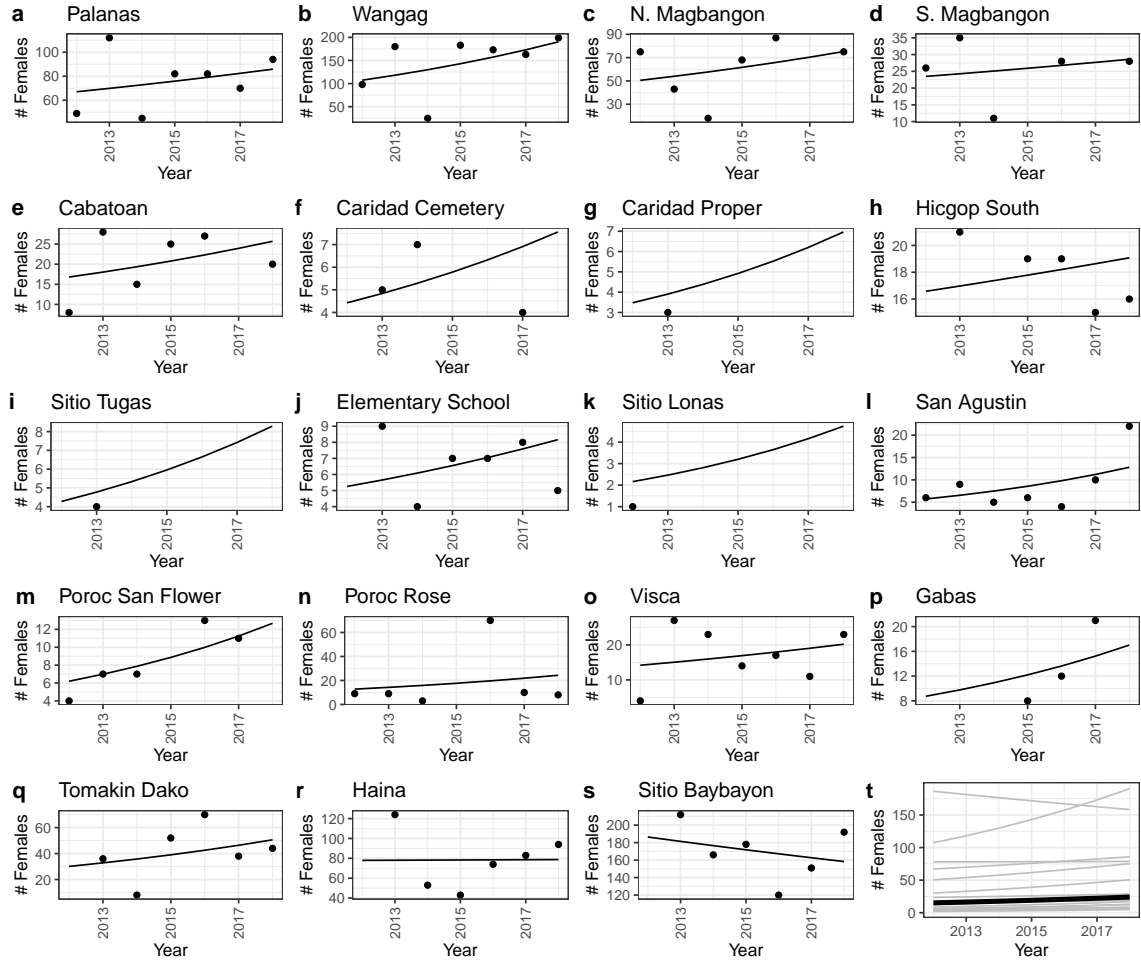


Figure D.7: Scaled number of females captured ( $F_{c_i,t}$ , black dots) and abundance trends (black lines) by patch from a mixed effects model with patch as a random effect.

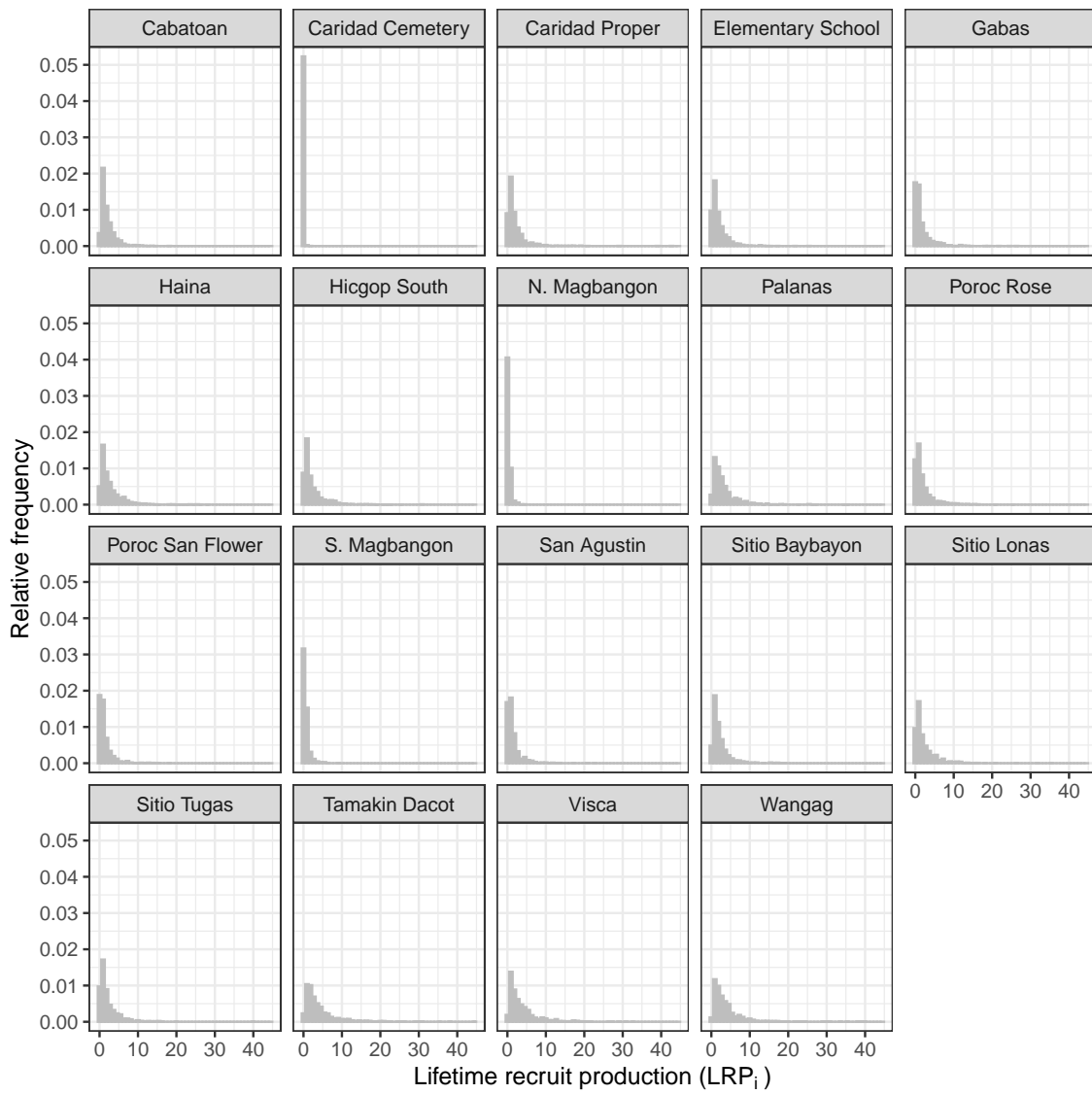


Figure D.8: Patch-specific lifetime recruit production ( $LRP_i$ ) estimates.

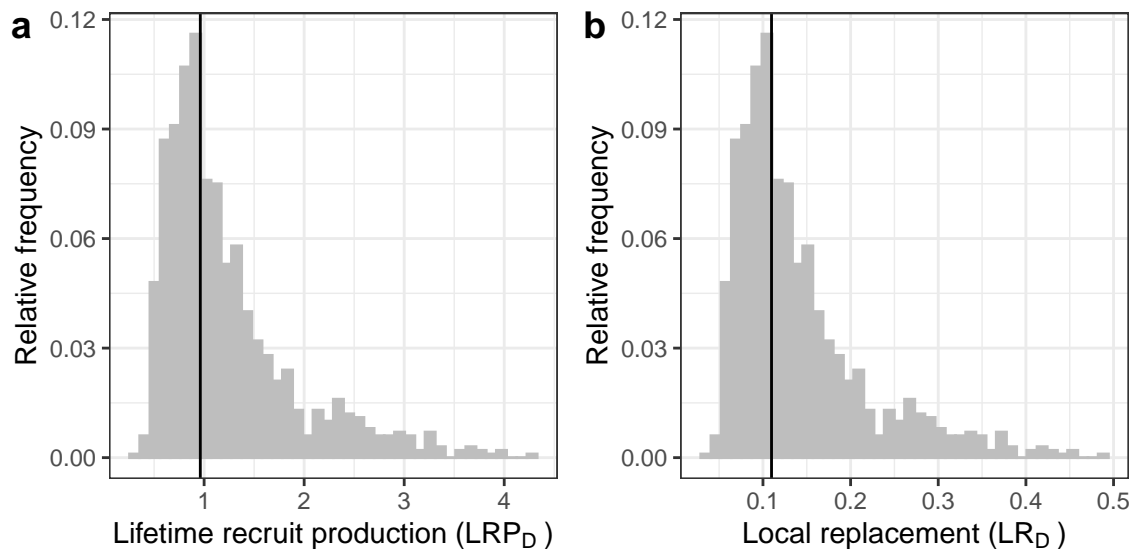


Figure D.9: Estimates of a) LRP averaged across patches, and b) local replacement without compensating for density dependence in early life stages in our data, showing the best estimate (black solid line) and range of estimates considering uncertainty (grey). These estimates compare to those in Fig. 4b and c, where we compensated for additional mortality in early life due to density dependence.

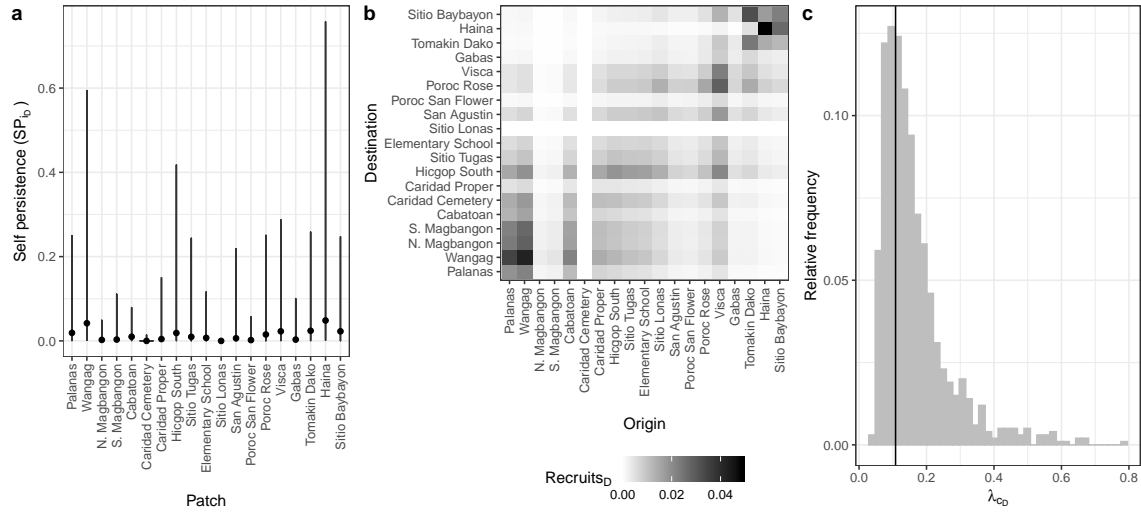


Figure D.10: Values of a) self-persistence ( $SP_{iD}$ ), b) realized connectivity among patches ( $C_{i,jD}$ ), and c) network persistence ( $\lambda_{cD}$ ) without compensation for density-dependence in early life stages in our data. For self-persistence (a) and network persistence (c), the best estimate is shown with in black (point for (a), line for (c)) and the range of estimates considering uncertainty is shown in grey. These estimates compare to those in Fig. 5 where we compensated for density dependence in early life stages.

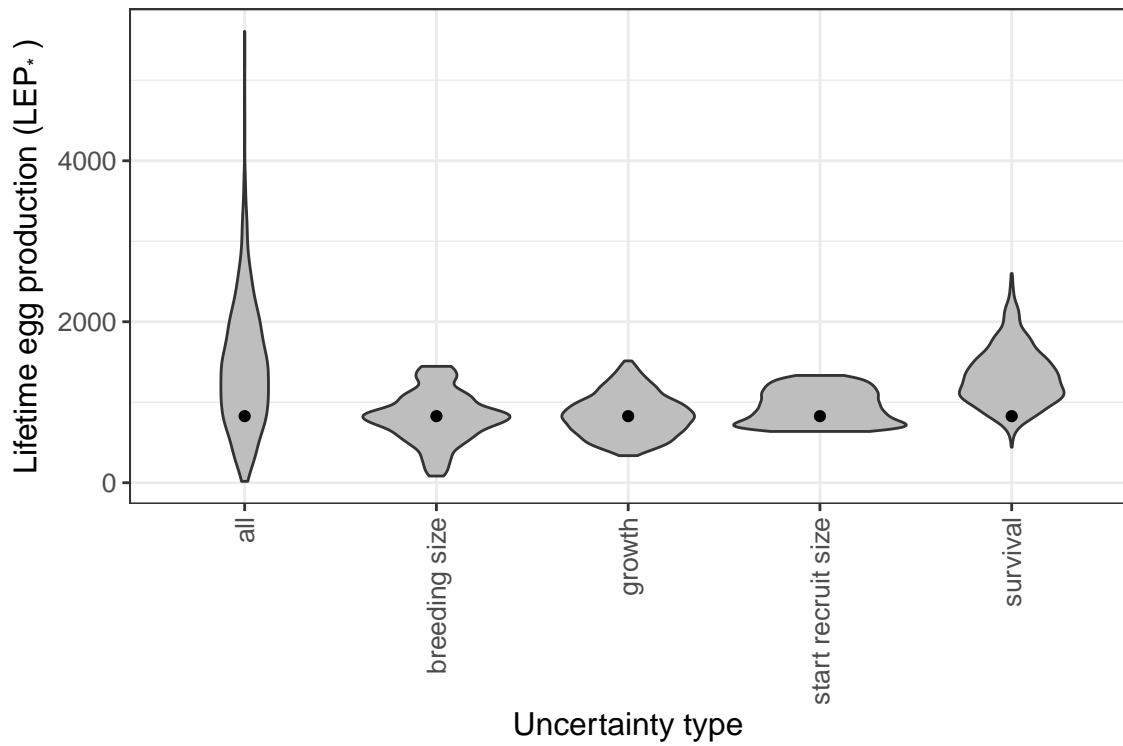


Figure D.11: The contribution of different sources of uncertainty in LEP averaged across patches ( $LEP_*$ ). We calculated the metrics using best estimates for all inputs except the one shown and show the results as violin plots, which show vertical probability densities of the metrics across a range of values.

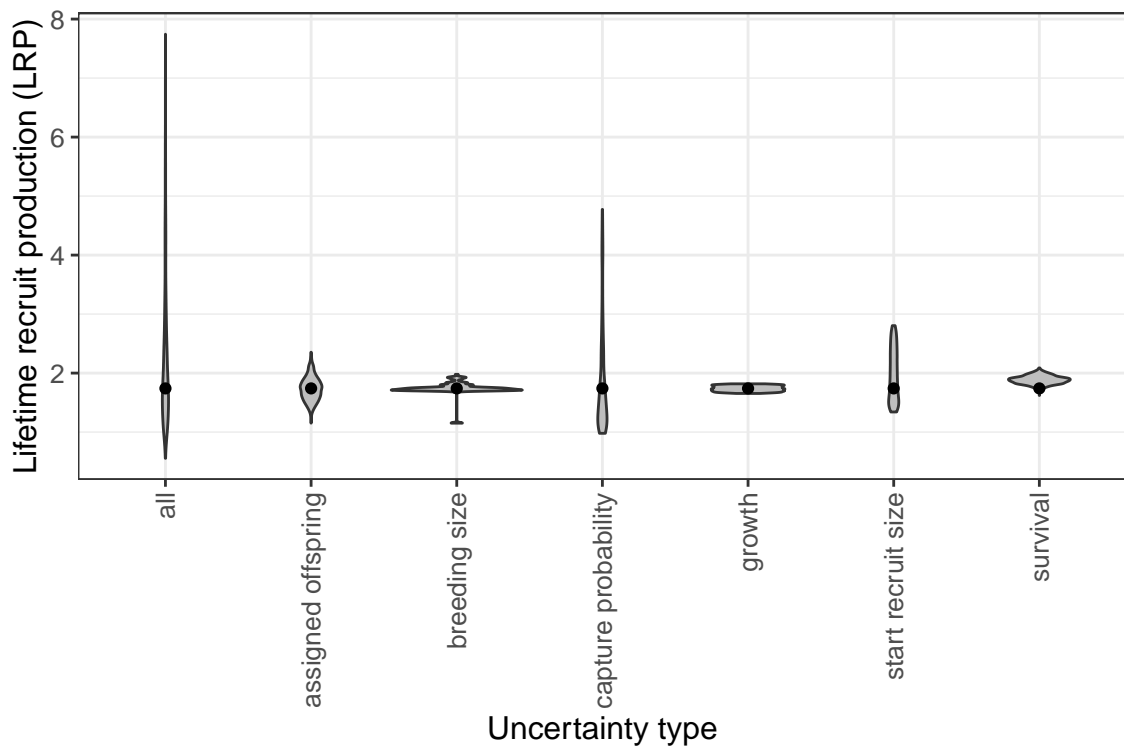


Figure D.12: The contribution of different sources of uncertainty in LRP averaged across patches. We calculated the metrics using best estimates for all inputs except the one shown and show the results as violin plots, which show vertical probability densities of the metrics across a range of values.

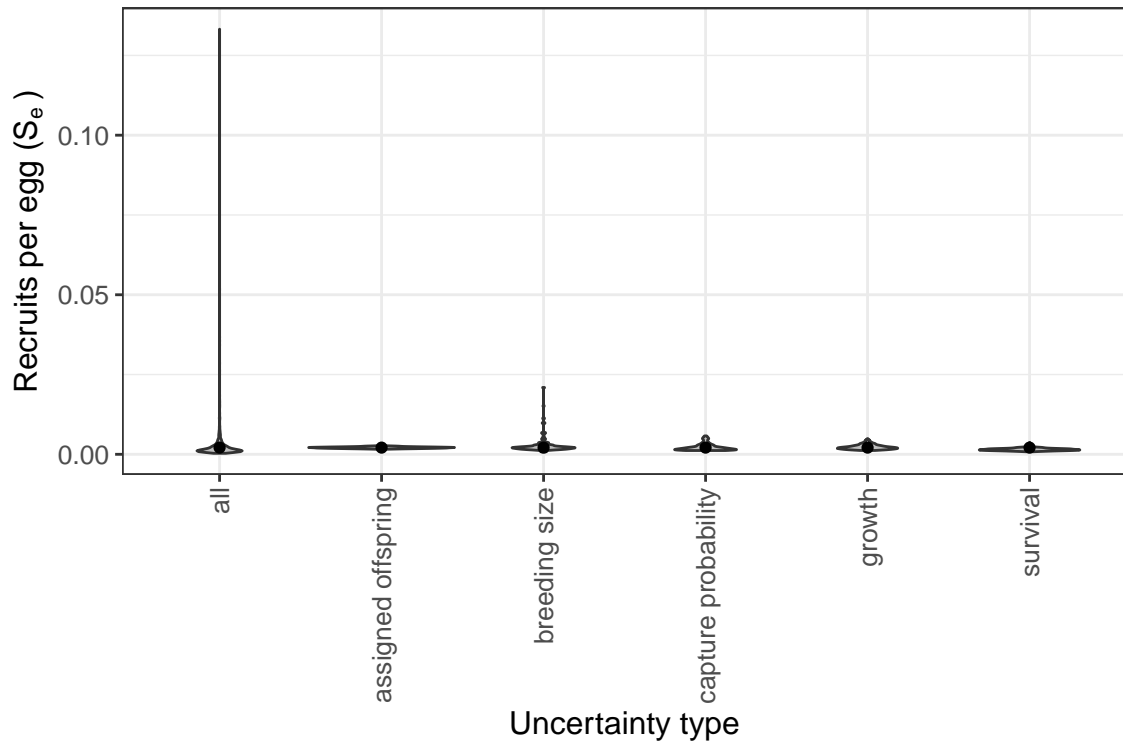


Figure D.13: The contribution of different sources of uncertainty in egg-recruit survival ( $S_e$ ). We calculated the metrics using best estimates for all inputs except the one shown and show the results as violin plots, which show vertical probability densities of the metrics across a range of values.

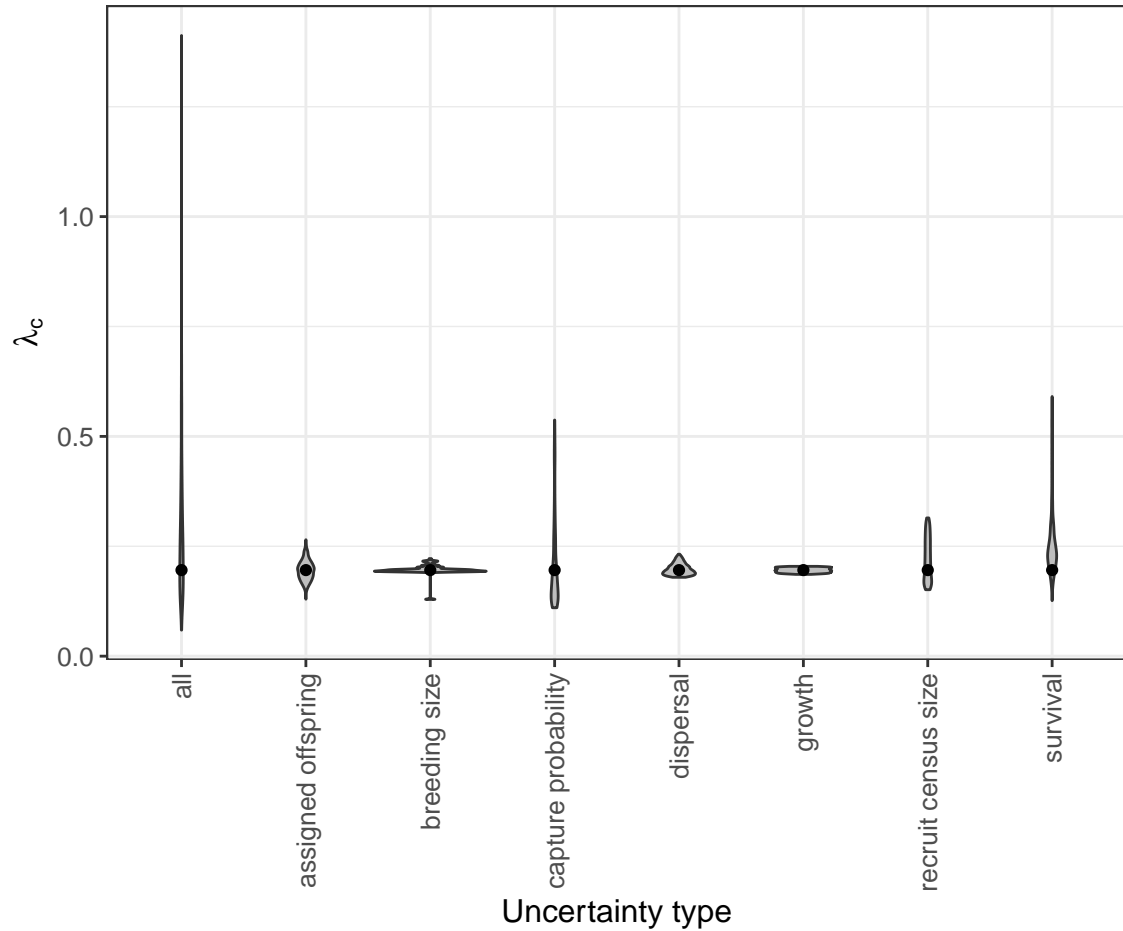


Figure D.14: The contribution of different sources of uncertainty in network persistence ( $\lambda_c$ ). We calculated the metrics using best estimates for all inputs except the one shown and show the results as violin plots, which show vertical probability densities of the metrics across a range of values.